Accepted Manuscript

New tetracyclic tacrine analogs containing pyrano[2,3-c]pyrazole: Efficient synthesis, biological assessment and docking simulation study

Mehdi Khoobi, Farzaneh Ghanoni, Hamid Nadri, Alireza Moradi, Morteza Pirali Hamedani, Farshad Homayouni Moghadam, Saeed Emami, Mohsen Vosooghi, Reza Zadmard, Alireza Foroumadi, Abbas Shafiee

PII: S0223-5234(14)00977-5

DOI: 10.1016/j.ejmech.2014.10.049

Reference: EJMECH 7457

To appear in: *European Journal of Medicinal Chemistry*

Received Date: 28 July 2014

Revised Date: 15 October 2014

Accepted Date: 16 October 2014

Please cite this article as: M. Khoobi, F. Ghanoni, H. Nadri, A. Moradi, M.P. Hamedani, F.H. Moghadam, S. Emami, M. Vosooghi, R. Zadmard, A. Foroumadi, A. Shafiee, New tetracyclic tacrine analogs containing pyrano[2,3-c]pyrazole: Efficient synthesis, biological assessment and docking simulation study, *European Journal of Medicinal Chemistry* (2014), doi: 10.1016/j.ejmech.2014.10.049.

Graphical abstract

New tetracyclic tacrine analogs containing pyrano[2,3-c]pyrazole: efficient synthesis, biological assessment and docking simulation study

Mehdi Khoobi, Farzaneh Ghanoni, Hamid Nadri, Alireza Moradi, Morteza Pirali Hamedani, Farshad Homayouni Moghadam, Saeed Emami, Mohsen Vosooghi, Reza Zadmard, Alireza Foroumadi, Abbas Shafiee*

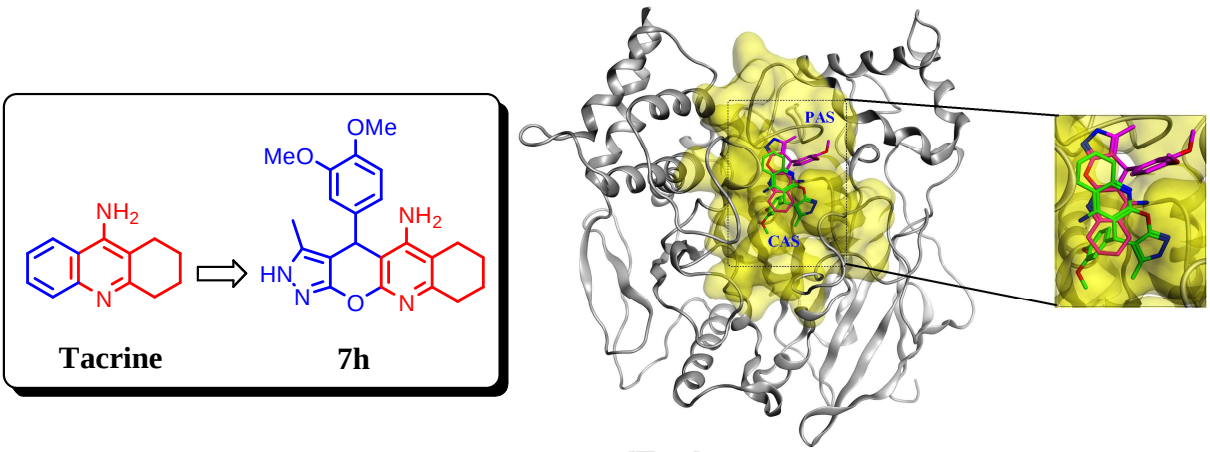

A new series of tacrine-based compounds **7a-l** were designed and synthesized as AChE inhibitors. The most potent compound **7h** bearing a 3,4-dimethoxyphenyl group was more active than reference drug tacrine.

New tetracyclic tacrine analogs containing pyrano[2,3-c]pyrazole: efficient synthesis, biological assessment and docking simulation study

Mehdi Khoobi[a], Farzaneh Ghanoni[b], Hamid Nadri[c], Alireza Moradi [c], Morteza Pirali Hamedani[a], Farshad Homayouni Moghadam[d], Saeed Emami[e], Mohsen Vosooghi[a], Reza Zadmard[b], Alireza Foroumadi[a], Abbas Shafiee[a,*]

[a] *Department of Medicinal Chemistry, Faculty of Pharmacy and Pharmaceutical Sciences Research Center, Tehran University of Medical Sciences, Tehran 14176, Iran*

[b] *Chemistry and Chemical Engineering Research Center of Iran (CCERCI), P. O. BOX 14335-186, Tehran, Iran*

[c] *Faculty of Pharmacy, Shahid Sadoughi University of Medical Sciences, Yazd, Iran*

[d] *Neurobiomedical Research Center, School of Medicine, Shahid Sadoughi University of Medical Sciences, Yazd, Iran*

[e] *Department of Medicinal Chemistry and Pharmaceutical Sciences Research Center, Faculty of Pharmacy, Mazandaran University of Medical Sciences, Sari, Iran*

Abstract: A new series of tacrine-based acetylcholinesterase (AChE) inhibitors **7a-l** were designed by replacing the benzene ring of tacrine with aryl-dihydropyrano[2,3-*c*]pyrazole. The poly-functionalized hybrid molecules **7a-l** were efficiently synthesized through multi-component reaction and subsequent Friedländer reaction between the obtained pyrano[2,3-*c*]pyrazoles and cyclohexanone. Most of target compounds showed potent and selective anti-AChE activity at sub-micromolar range. The most potent compound **7h** bearing a 3,4-dimethoxyphenyl group was more active than reference drug tacrine. The representative compound **7h** could significantly protect neurons against oxidative stress as potent as quercetin at low concentrations. The docking study of compound **7h** with AChE enzyme revealed that the (*R*)-enantiomer binds preferably to CAS while the (*S*)-enantiomer prone to be a PAS binder.

Keywords: Alzheimer's disease; Acetylcholinesterase; Docking study; Neuroprotective activity; Tacrine

* Corresponding author. Tel: +98 21 66406757; Fax: +98 21 66461178.
E-mail address: ashafiee@ams.ac.ir (A. Shafiee).

1. Introduction

Alzheimer's disease (AD) is a complex and multifactorial age-related neurodegenerative disorder characterized by progressive loss of memory, attention, language skills, along with depression [1]. Several factors including decline of acetylcholine (ACh), *β*-amyloid (A*β*) deposits, τ-protein (τ) aggregation, oxidative stress, and imbalance of bio-metals have been proposed to explain the mechanism of AD pathogenesis [2].

The previous studies have demonstrated that the inhibition of AChE which resulted in rising the ACh level in brain, is a desirable approach in the treatment of AD [3]. Also, it was proposed that the peripheral anionic site (PAS) of AChE involves in the aggregation of amyloid fibrils [4]. Consequently, the finding of AChE inhibitors which simultaneously bind to both catalytic and peripheral binding sites has become a very active area for design and development of anti-Alzheimer's disease drugs [5]. On the other hand, oxidative damages may accelerate the appearance of amyloid plaques and neurofibrillary (NFT) tangles in the brain [6]. Therefore, preventing the formation of the free radicals or protecting against oxidative stress by neuroprotective agents may be a suitable approach for AD therapy [7].

Tacrine (9-amino-1,2,3,4-tetrahydroacridine) is a AChE inhibitor that proved to have a beneficial effect in patients with mild-to-moderate dementia of AD [8]. Unfortunately, the administration of tacrine for the treatment of AD associated with high incidence of hepatotoxicity [9]. Modifications on the tacrine structure have been mainly focused on the replacement of the benzene ring in tacrine by a heterocyclic ring, and also tacrine-based molecular hybridizations. Thomae et al. reported different analogs where the benzene ring in tacrine was replaced by thiophene, thiazole, 4-azaisoindole, or selenophene heterocycles [10-13]. Futhermore, Tzeng and co-workers synthesized a few substituted benzofuro[2,3-*b*]quinoline derivatives as tetracyclic analogs of tacrine [14].

In the search for finding multi-targeted AChE inhibitors, Marco-Contelles et al. have designed a series of 1,8-naphthyridine derivatives related to tacrine. [15]. Tacrine analog **A** (Fig. 1), the best AChE inhibitor of this series, exhibited neuroprotective activity against oxidative stress induced by two toxic insults of the mitochondrial chain. The same group also reported tacrine analogs, such as pyrazolo[3,4-*b*]quinoline and benzo[*b*]pyrazolo[4,3-*g*][1,8]naphthyridine derivatives, as potent and selective AChE inhibitors. Particularly, compound **B** was able to protect SH-SY5Y cells against two toxic molecules (rotenone/oligomicin-A) [16].

Recently, a series of benzochromene-based tacrines namely 7-aryl-9,10,11,12-tetrahydro-7*H*-benzo[7,8]chromeno[2,3-*b*]quinolin-8-amines were synthesized and evaluated as potent and selective inhibitors of AChE [17,18]. Among them, tacrine-like compound **C** had an excellent antioxidant profile and significant neuroprotective effects in cortical neurons against mitochondrial chain blocker-induced cell death.

As described above, AD is a complex disease which could be better managed by agents acting upon more than one target. Considering this strategy and in continue of our previous works on anti-AChE agents [19], we designed a novel series of tacrine-based compounds consisting pyrano[2,3-*c*]pyrazole substructure. Since the pyrazole and 4-substituted pyran were found in the reported compounds **B** and **C**, they were incorporated in the tacrine scaffold to achieve new entity 2,4,6,7,8,9-hexahydropyrazolo[4',3':5,6]pyrano[2,3-*b*]quinolin-5-amines (**7a-l**). Thus we described here, synthesis, in vitro anti-cholinesterase and neuroprotective evaluation and in silico study of tacrine-based compounds **7a-l** containing pyrano[2,3-*c*]pyrazole system.

2. Chemistry

As illustrated in Scheme 1, target compounds **7** were easily prepared in two steps. Initially, preparation of pyrano[2,3-*c*]pyrazoles **5** [20] via one-pot four-component reaction of ethylacetoacetate (**1**), hydrazine hydrate (**2**), malononitrile (**3**) and 4-methylbenzaldehyde (**4a**) was studied under several conditions. Several catalysts [(*S*)-proline, piperidine, pyridine, NaOH, K_2CO_3] and various environmentally benign solvents (water, EtOH and polyethylene glycol) were investigated to find the best condition. After optimization, the best results in terms of yield were achieved by using of (*S*)-proline in water-ethanol medium (1:1) under reflux condition (isolated yield was 81%). Ultrasonic is an alternative mode of energy to accelerate the reaction time and even improve the yield of the reaction. Therefore, the model reaction was screened under ultrasonic irradiation to find the best reaction condition. The results of this comparative experiment showed that application of ultrasonic irradiation cause to shorten the reaction time up to 20 min and improve the yield of the reaction up to 92% at room temperature. In the next step, $AlCl_3$ catalyzed Friedländer reaction between the obtained pyrano[2,3-*c*]pyrazoles **5** and cyclohexanone (**6**) resulted in the formation of target products **7**.

It should be noted that intermediates **5a-l** and target compounds **7a-l** were obtained as a mixture of enantiomers, having no detectable optical activity.

3. Results and discussion

3.1. Pharmacology

3.1.1. Anti-cholinesterase activity

The anti-cholinesterase activity of target compounds **7a-l** was assessed in vitro against AChE from *Electrophorus electricus* (*eel*AChE) and horse serum butyrylcholinesterase (*eq*BuChE) in comparison to tacrine as reference drug. The results were presented in Table 1, as IC_{50} values in µM. The obtained IC_{50} values revealed that all tested compounds with exception of **7f** showed significant inhibitory activity against AChE (IC_{50} values = 0.19-3.27 µM). The most active compound was 3,4-dimethoxyphenyl derivative **7h** with IC_{50} value of 0.19 µM. Its anti-AChE activity was superior to that of reference drug tacrine. Furthermore, 4-methoxyphenyl analog **7e** and 1-naphthyl derivative **7k** were practically as potent as tacrine against AChE.

The IC_{50} values of 4-substituted phenyl analogs **7a**, **7c** and **7e** revealed that the methoxy group on *para*-position of phenyl ring is more favorable than methyl or fluoro substituents. The introduction of second methoxy group on 4-methoxyphenyl residue of compound **7e**, resulted in compound **7h** with improved anti-AChE activity. However, the insertion of third methoxy group on phenyl ring diminished the activity, as observed in compound **7i**. Surprisingly, while the 2-methoxyphenyl analog **7f** was inactive against AChE, but 2,5-dimethoxyphenyl derivative **7g** had potent activity with IC_{50} value of 0.5 µM. The sub-micromolar activity of compound **7k** showed that the bicyclic 1-naphthyl group is truly tolerated on the pyran part of the molecule.

In terms of anti-BuChE activity, only compounds **7a-c**, **7k** and **7l** showed inhibitory activity and remaining compounds were inactive. 4-Tolyl derivative **7a** with IC_{50} value of 4.5 µM was the most potent compound against BuChE. The data obtained for inhibition of AChE/BuChE by target compounds **7a-l** demonstrated that most compounds had high selectivity for AChE over BuChE. However, compound **7a** with selectivity index of 6 had the lowest selectivity.

3.1.2. Kinetic analysis of AChE inhibition

The kinetic studies were performed using the most active compound **7h** to understand the kinetic of the inhibition on AChE. The inhibition kinetic of compound **7h** using Lineweaver-Burk plot was depicted in Fig. 2. As interpreted from the pattern of inhibition in Fig. 2, the mechanism of

action on AChE for compound **7h** is a mixed-type inhibition. The K_i value of compound **7h** was calculated (K_i= 0.49 µM) using Lineweaver-Burk secondary plot (Fig. 3).

3.1.3. Neuroprotection against H_2O_2-induced cell death in PC12 cells

The most potent compound against AChE (**7h**) was further subjected to in vitro neuroprotective assay against H_2O_2-induced damage in PC12 cells. The data are summarized in Fig. 4 in which the percent of cell viability was calculated in comparison with control group. The tested concentrations were selected according to the non-toxic range (<15 µM) of the **7h** against PC12 cells. Based on the results, compound **7h** showed significant neuroprotective activity at 10 µM (viability= 48.35%) that is comparable with quercetin at the same concentration (viability= 51.63%).

3.2. Ligand-protein docking simulation

The molecular docking study was performed to understand the binding interactions of designed compounds at the molecular level. Since the final compounds have a chiral center at the 4-position of pyran ring, they are racemic mixtures. Thus, both (*R*)- and (*S*)-enantiomers were studied in docking simulations. The preliminary analysis of docking results by visual inspection showed that the best poses of target compounds **7a-l** were docked similarly. Therefore, the best pose of compound (*R,S*)-**7h** as a promising compound was further analyzed in detail.

As shown in Fig. 5, the orientation of (*R*)- and (*S*)-enantiomers was different in the gorge of the enzyme. The (*R*)-enantiomer was placed at the bottom of the gorge in the vicinity of catalytic triad while the (*S*)-enantiomer occupied the bottle-neck of the gorge adjacent to peripheral anionic site (PAS). Moreover, according to the interaction mode of the both (*R*)- and (*S*)-enantiomers, it seems that aminopyridine moiety play an important role in ligand recognition via π–π stacking with Tyr334. In the case of (*R*)-enantiomer (Fig. 6), after anchoring of the ligand through aforementioned interaction, the dimethoxyphenyl moiety oriented toward the catalytic anionic subsite (CAS). In this position, the dimethoxyphenyl moiety was well accommodated in the CAS through a T-shape π–π stacking with Phe330 and hydrogen binding with His440. In addition, the second methoxy was set alongside the oxyanion hole. In such orientation, the (*S*)-enantiomer could not well accommodate due to steric clash with Trp84. Thereupon, it turned reversely toward PAS to relieve this clash leading to formation of the following interactions: a T-

shape π–π stacking of dimethoxyphenyl with Trp279 and a hydrogen bond between pyrazole ring and Ser286 (Fig. 7). It could be concluded that the (*R*)-enantiomer binds preferably to CAS while the (*S*)-enantiomer prone to be a PAS binder.

4. Conclusion

In the search for finding new potential anti-cholinesterase agents, we replaced the benzene ring of tacrine by aryl-dihydropyrano[2,3-*c*]pyrazole. The poly-functionalized hybrid molecules **7a-l** were efficiently synthesized through multi-component reaction and subsequent Friedländer reaction between the obtained pyrano[2,3-*c*]pyrazoles and cyclohexanone. Most of target compounds showed potent and selective anti-AChE activity at sub-micromolar levels.

The structure-activity relationship study revealed that the potency profile against AChE/BuChE could be modulated properly by altering the substitutions on the phenyl group attached to the dihydropyran substructure. Compound **7h** bearing a 3,4-dimethoxyphenyl group was the most potent compound against AChE, being more active than reference drug tacrine. The in vitro neuroprotective assay of compound **7h** against H_2O_2-induced damage in PC12 cells demonstrated that the tested compound could significantly protect neurons against oxidative stress as potent as quercetin at low concentrations. The docking study of compound **7h** with AChE enzyme revealed that the (*R*)-enantiomer binds preferably to CAS while the (*S*)-enantiomer prone to be a PAS binder. The high potency and selectivity of the representative compound **7h**, along with its significant neuroprotective effects against oxidative stress and potential binding of its (*S*)-enantiomer to the PAS reserved it as a lead for AD therapy.

5. Experimental

5.1. General chemistry

All commercially available reagents were used without further purification. TLC was conducted on silica gel 250 micron, F254 plates. Melting points were measured on a Kofler hot stage apparatus and are uncorrected. The IR spectra were taken using Nicolet FT-IR Magna 550 spectrograph (KBr discs). ^{1}H NMR spectra were recorded on Brucker 400 MHz NMR instruments. The chemical shifts (δ) and coupling constants (J) are expressed in parts per million and Hertz, respectively. The atoms numbering of the target compounds used for ^{1}H NMR data

are shown in Scheme 1. Mass spectra of the products were obtained with an HP (Agilent technologies) 5937 Mass Selective Detector. Elemental analyses were carried out by a CHN-Rapid Heraeus elemental analyzer. The results of elemental analyses (C, H, N) were within ±0.4% of the calculated values.

*5.2. General procedure for the preparation of pyrano[2,3-c]pyrazole derivatives (**5**)*

In a 100 mL round bottom flask, a mixture of hydrazine hydrate (12 mmol), ethyl acetoacetate (10 mmol), malononitrile (10 mmol), (*S*)-proline (10% mol) and water (20 mL) were taken and the mixture was irradiated in the ultrasonic bath for 2 min. Afterward, aromatic aldehyde (10 mmol) was added to the mixture and the mixture was irradiated for 10-30 min. Progress of the reaction was monitored by TLC. After completion of the reaction, the precipitated solid was filtered and further purified by recrystallization from ethanol.

*5.3. General procedure for the preparation of compounds **7a-l***

This procedure was carried out according to our previous reported method [21]. Briefly, aluminium chloride (1.5 equiv.) was suspended in dry 1,2-dichloroethane (10 mL) at room temperature under argon atmosphere. After stirring the suspension for a few minutes, the corresponding pyrano[2,3-*c*]pyrazole (1 equiv.) and cyclohexanone (1.5 equiv.) were added to the mixture and the reaction mixture was heated under reflux for 24 h. Progress of the reaction was monitored by TLC. After completion of the reaction, an aqueous solution of sodium hydroxide (10%) was added dropwise to the mixture until the aqueous solution became basic. After stirring for 30 min, the precipitate was filtered and washed with water.

*5.3.1. 3-Methyl-4-(p-tolyl)-2,4,6,7,8,9-hexahydropyrazolo[4',3':5,6]pyrano[2,3-b]quinolin-5-amine (**7a**).* Yield 92%; white solid; mp >250 ºC; IR (KBr, cm^{-1}) ν_{max}: 3391 and 3191 (NH_2), 1581 (C=N). ^{1}H NMR (DMSO-d_6, 400 MHz) δ: 12.04 (bs, 1H, NH), 7.12 (d, 2H, J = 8.0 Hz, $H_{2,6\ phenyl}$), 7.03 (d, 2H, J = 8.0 Hz, $H_{3,5\ phenyl}$), 5.30 (bs, 2H, NH_2), 5.12 (s, 1H, H_4), 2.57 (bs, 2H, $2H_9$), 2.50 (s, 3H, $CH_{3\ phenyl}$), 2.34-2.20 (bs, 2H, $2H_6$), 1.96 (s, 3H, $CH_{3\ pyrazol}$), 1.66 (bs, 4H, $2H_7$ and $2H_8$). ^{13}C NMR (DMSO-d_6, 100 MHz) δ: 175.4, 156.1, 152.6, 152.4, 142.5, 135.6, 129.3, 127.6, 112.4, 100.2, 99.0, 34.3, 32.4, 25.3, 23.3, 22.8, 22.5, 10.2. Anal. Calcd for $C_{21}H_{22}N_4O$: C, 72.81; H, 6.40; N, 16.17. Found: C, 72.53; H, 6.63; N, 15.08.

*5.3.2. 4-(2-Fluorophenyl)-3-methyl-2,4,6,7,8,9-hexahydropyrazolo[4',3':5,6]pyrano[2,3-b]quinolin-5-amine (**7b**).* Yield 86%; white solid; mp >250 ºC; IR (KBr, cm^{-1}) ν_{max}: 3494 and 3407 (NH_2), 1585 (C=N). ^{1}H NMR (DMSO-d_6, 400 MHz) δ: 11.90 (bs, 1H, NH), 7.36 (t, 1H, J = 7.2 Hz, H_{phenyl}), 7.21-7.20 (m 1H, H_{phenyl}), 7.11-7.04 (m, 2H, H_{phenyl}), 5.34 (s, 1H, H_4), 5.20 (bs, 2H, NH_2), 2.57 (bs, 2H, $2H_9$), 2.33-2.16 (m, 2H, $2H_6$), 1.95 (s, 3H, $CH_{3\ pyrazol}$), 1.69 (bs, 4H, $2H_7$ and $2H_8$). ^{13}C NMR (DMSO-d_6, 100 MHz) δ: 161.4, 158.9, 157.1, 156.1, 152.8, 152.3, 135.4, 131.3, 131.2, 130.5, 130.4, 129.0, 128.9, 124.9, 116.3, 112.2, 98.5, 97.7, 32.4, 29.7, 23.3, 22.7, 22.5, 9.9. Anal. Calcd for $C_{20}H_{19}FN_4O$: C, 68.56; H, 5.47; N, 15.99. Found: C, 68.21; H, 5.18; N, 15.72.

*5.3.3. 4-(4-Fluorophenyl)-3-methyl-2,4,6,7,8,9-hexahydropyrazolo[4',3':5,6]pyrano[2,3-b]quinolin-5-amine (**7c**).* Yield 88%; white solid; mp >250 ºC; IR (KBr, cm^{-1}) ν_{max}: 3505 and 3385 (NH_2), 1586 (C=N). ^{1}H NMR (DMSO-d_6, 400 MHz) δ: 11.90 (bs, 1H, NH), 7.28-7.25 (m, 2H, $H_{3,5\ phenyl}$), 7.08-7.04 (m, 2H, $H_{2,6\ phenyl}$), 5.41 (bs, 2H, NH_2), 5.23 (s, 1H, H_4), 2.57 (bs, 2H, $2H_9$), 2.33-2.16 (m, 2H, $2H_6$), 1.99 (s, 3H, CH_3 pyrazol), 1.70 (bs, 4H, $2H_7$ and $2H_8$). ^{13}C NMR (DMSO-d_6, 100 MHz) δ: 162.2, 159.8, 156.7, 156.0, 152.7, 152.2, 141.7, 141.6, 135.3, 129.5, 115.6, 115.4, 112.5, 100.1, 98.8, 33.7, 32.3, 23.3, 22.7, 22.5, 10.2. Anal. Calcd for $C_{20}H_{19}FN_4O$: C, 68.56; H, 5.47; N, 15.99. Found: C, 68.79; H, 5.79; N, 16.22.

*5.3.4. 3-Methyl-4-(3-nitrophenyl)-2,4,6,7,8,9-hexahydropyrazolo[4',3':5,6]pyrano[2,3-b]quinolin-5-amine (**7d**).* Yield 94%; yellow solid; mp >250 ºC; IR (KBr, cm^{-1}) ν_{max}: 3411 and 3368 (NH_2), 1583 (C=N). ^{1}H NMR (DMSO-d_6, 400 MHz) δ: 11.9 (bs, 1H, NH), 8.24 (s, 1H, $H_{2\ phenyl}$), 8.00 (d, 1H, J = 8.0 Hz, $H_{4\ phenyl}$), 7.60-7.51 (m, 2H, $H_{5,6\ phenyl}$), 5.57 (bs, 2H, NH_2), 5.45 (s, 1H, H_4), 2.58 (bs, 2H, $2H_9$), 2.35-2.13 (m, 2H, $2H_6$), 2.00 (s, 3H, CH_3 pyrazol), 1.69 (bs, 4H, $2H_7$ and $2H_8$). ^{13}C NMR (DMSO-d_6, 100 MHz) δ: 156.8, 156.0, 153.4, 152.6, 148.0, 147.8, 135.6, 134.4, 130.5, 122.1, 121.0, 112.6, 99.4, 98.1, 33.8, 32.4, 23.3, 22.7, 22.5, 10.2. Anal. Calcd for $C_{20}H_{19}N_5O_3$: C, 63.65; H, 5.07; N, 18.56. Found: C, 63.34; H, 5.26; N, 18.21.

*5.3.5. 4-(4-Methoxyphenyl)-3-methyl-2,4,6,7,8,9-hexahydropyrazolo[4',3':5,6]pyrano[2,3-b]quinolin-5-amine (**7e**).* Yield 93%; white solid; mp >250 ºC; IR (KBr, cm^{-1}) ν_{max}: 3493 and 3403 (NH_2), 1574 (C=N). ^{1}H NMR (DMSO-d_6, 400 MHz) δ: 11.84 (bs, 1H, NH), 7.16 (d, 2H, J = 8.4 Hz, $H_{2,6\ phenyl}$), 6.80 (d, 2H, J = 8.4 Hz, $H_{3,5\ phenyl}$), 5.29 (bs, 2H, NH_2), 5.10 (s, 1H, H_4), 3.39 (s, 3H, OCH_3), 2.57 (bs, 2H, $2H_9$), 2.32-2.19 (m, 2H, $2H_6$), 1.98 (s, 3H, CH_3 pyrazol), 1.70 (bs, 4H, $2H_7$ and $2H_8$). ^{13}C NMR (DMSO-d_6, 100 MHz) δ: 158.0, 156.8, 156.0, 152.6, 137.5, 135.2, 128.7, 114.2, 112.4, 100.5, 99.1, 55.4, 33.8, 32.4, 23.3, 22.8, 22.5, 10.2. Anal. Calcd for $C_{21}H_{22}N_4O_2$: C, 69.59; H, 6.12; N, 15.46. Found: C, 69.21; H, 6.48; N, 15.12.

*5.3.6. 4-(2-Methoxyphenyl)-3-methyl-2,4,6,7,8,9-hexahydropyrazolo[4',3':5,6]pyrano[2,3-b]quinolin-5-amine (**7f**).* Yield 81%; white solid; mp >250 ºC; IR (KBr, cm^{-1}) ν_{max}: 3431 and 3375 (NH_2), 1582 (C=N). ^{1}H NMR (DMSO-d_6, 400 MHz) δ: 11.95 (bs, 1H, NH), 7.03-6.83 (m, $4H_{phenyl}$), 5.31 (s, 1H, H_4), 5.16 (bs, 2H, NH_2), 3.69 (s, 3H, OCH_3), 2.49 (bs, 2H, $2H_9$), 2.24-2.19 (m, 2H, $2H_6$), 1.96 (s, 3H, CH_3 pyrazol), 1.68 (bs, 4H, $2H_7$ and $2H_8$). ^{13}C NMR (DMSO-d_6, 100 MHz) δ: 157.3, 156.3, 152.4, 150.8, 136.8, 134.6, 126.4, 125.1, 122.3, 114.2, 112.6, 100.0, 99.6, 54.8, 33.5, 32.2, 23.1, 22.6, 22.3, 10.1. Anal. Calcd for $C_{21}H_{22}N_4O_2$: C, 69.59; H, 6.12; N, 15.46. Found: 69.76; H, 6.32; N, 15.68.

*5.3.7. 4-(2,5-Dimethoxyphenyl)-3-methyl-2,4,6,7,8,9-hexahydropyrazolo[4',3':5,6]pyrano[2,3-b]quinolin-5-amine (**7g**).* Yield 88%; yellow solid; mp >250 ºC; IR (KBr, cm^{-1}) ν_{max}: 3448 and 3374 (NH_2), 1586 (C=N). ^{1}H NMR (DMSO-d_6, 400 MHz) δ: 11.86 (bs, 1H, NH), 6.97 (d, 1H, J = 8.5 Hz, $H_{3\ phenyl}$), 6.75-6.73 (m, 1H, $H_{4\ phenyl}$), 6.35 (bs, 1H, $H_{6\ phenyl}$), 5.27 (s, 1H, H_4), 5.22 (bs, 2H, NH_2), 3.83 (s, 3H, OCH_3), 3.56 (s, 3H, OCH_3), 2.51-2.26 (m, 4H, $2H_9$ and $2H_6$), 1.89 (s, 3H, CH_3 pyrazol), 1.69 (bs, 4H, $2H_7$ and $2H_8$). ^{13}C NMR (DMSO-d_6, 100 MHz) δ: 157.9, 156.0, 154.0, 152.6, 152.2, 149.8, 135.2, 134.1, 116.2, 112.6, 112.2, 11.8, 99.6, 98.9, 56.8, 55.6, 45.5, 32.3, 23.2, 22.7, 22.5, 9.8. Anal. Calcd for $C_{22}H_{24}N_4O_3$: C, 67.33; H, 6.16; N, 14.28. Found: C, 67.58; H, 6.43; N, 14.01.

*5.3.8. 4-(3,4-Dimethoxyphenyl)-3-methyl-2,4,6,7,8,9-hexahydropyrazolo[4',3':5,6]pyrano[2,3-b]quinolin-5-amine (**7h**).* Yield 90%; white solid; mp >250 ºC; IR (KBr, cm^{-1}) ν_{max}: 3481 and 3389 (NH_2), 1584 (C=N).). ^{1}H NMR (DMSO-d_6, 400 MHz) δ: 11.86 (bs, 1H, NH), 7.05 (d, 1H, J = 2.0 Hz, $H_{2\ phenyl}$), 6.80 (d, 1H, J = 8.4 Hz, $H_{5\ phenyl}$), 6.59 (dd, 1H, J = 8.4 and J = 2.0 Hz, $H_{6\ phenyl}$), 5.30 (bs, 2H, NH_2), 5.08 (s, 1H, H_4), 3.68 (s, 3H, OCH_3), 3.66 (s, 3H, OCH_3), 2.57 (bs, 2H, $2H_9$), 2.32-2.17 (m, 2H, $2H_6$), 2.02 (s, 3H, CH_3 pyrazol), 1.70 (bs, 4H, $2H_7$ and $2H_8$). ^{13}C NMR (DMSO-d_6, 100 MHz) δ: 156.7, 156.0, 152.7, 152.5, 148.7, 147.5, 138.0, 135.3, 119.6, 112.5, 112.3, 112.1, 100.3, 98.9, 55.9, 55.8, 34.3, 32.4, 23.3, 22.8, 22.5, 10.3. Anal. Calcd for $C_{22}H_{24}N_4O_3$: C, 67.33; H, 6.16; N, 14.28. Found: C, 67.55; H, 5.89; N, 14.54.

*5.3.9. 3-Methyl-4-(3,4,5-trimethoxyphenyl)-2,4,6,7,8,9-hexahydropyrazolo[4',3':5,6]pyrano[2,3-b]quinolin-5-amine (**7i**).* Yield 95%; yellow solid; mp >250 ºC; IR (KBr, cm^{-1}) ν_{max}: 3483 and 3383 (NH_2), 1590 (C=N). ^{1}H NMR (DMSO-d_6, 400 MHz) δ: 11.90 (bs, 1H, NH), 6.57 (s, 2H, $H_{2,6\ phenyl}$), 5.46 (s, 1H, H_4), 5.12 (bs, 2H, NH_2), 3.72 (s, 6H, 2×OCH_3), 3.65 (s, 3H, OCH_3), 2.50 (bs, 2H, $2H_9$), 2.09 (bs, 2H, $2H_6$), 2.05 (s, 3H, CH_3 pyrazol), 1.71 (bs, 4H, $2H_7$ and $2H_8$). ^{13}C NMR (DMSO-d_6, 100 MHz) δ: 156.2, 155.4, 152.7, 140.6, 135.8, 134.9, 111.9, 104.7, 99.5, 98.1, 59.9, 55.8, 34.5, 31.6, 22.8, 22.2, 22.0, 9.9. Anal. Calcd for $C_{23}H_{26}N_4O_4$: C, 65.39; H, 6.20; N, 13.26. Found: C, 65.67; H, 6.51; N, 13.01.

*5.3.10. 4-(2,3-Dichlorophenyl)-3-methyl-2,4,6,7,8,9-hexahydropyrazolo[4',3':5,6]pyrano[2,3-b]quinolin-5-amine (**7j**).* Yield 82%; white solid; mp >250 ºC; IR (KBr, cm^{-1}) ν_{max}: 3477 and 3343 (NH_2), 1586 (C=N). ^{1}H NMR (DMSO-d_6, 400 MHz) δ: 11.99 (bs, 1H, NH), 7.62 (d, J = 8.9 Hz, $H_{4\ phenyl}$), 7.49 (t, J = 8.9 Hz, $H_{5\ phenyl}$), 7.28 (d, J = 8.9 Hz, $H_{6\ phenyl}$), 5.56 (s, 1H, H_4), 5.07 (bs, 2H, NH_2), 2.56 (bs, 2H, $2H_9$), 2.36 (bs, 2H, $2H_6$), 1.96 (s, 3H, CH_3 pyrazol), 1.77 (bs, 4H, $2H_7$ and $2H_8$). ^{13}C NMR (DMSO-d_6, 100 MHz) δ: 157.1, 156.2, 153.3, 152.4, 135.7, 132.4, 130.7, 130.1, 129.7, 129.5, 129.2, 112.8, 98.1, 32.4, 23.3, 22.8, 22.4, 10.3. Anal. Calcd for $C_{20}H_{18}Cl_2N_4O$: C, 59.86; H, 4.52; N, 13.96. Found: C, 59.51; H, 4.26; N, 13.68.

*5.3.11. 3-Methyl-4-(naphthalen-1-yl)-2,4,6,7,8,9-hexahydropyrazolo[4',3':5,6]pyrano[2,3-b]quinolin-5-amine (**7k**).* Yield 78%; white solid; mp >250 ºC; IR (KBr, cm^{-1}) ν_{max}: 3419 and 3321 (NH_2), 1585 (C=N). ^{1}H NMR (DMSO-d_6, 400 MHz) δ: 11.92 (bs, 1H, NH), 7.97 (bs, 1H,

$H_{naphtyl}$), 7.84-7.75 (m, 3H, $H_{naphtyl}$), 7.49-7.42 (m, 2H, $H_{naphtyl}$), 7.21 (d, 1H, J = 8.4 Hz, $H_{naphtyl}$), 5.38 (s, 1H, H_4), 5.36 (bs, 2H, NH_2), 2.59 (bs, 2H, $2H_9$), 2.31-2.12 (m, 2H, $2H_6$), 1.97 (s, 3H, CH_3 pyrazol), 1.68 (bs, 4H, $2H_7$ and $2H_8$). ^{13}C NMR (DMSO-d_6, 100 MHz) δ: 156.8, 156.1, 152,9, 152.6, 142.6, 135.6, 133.1, 132.2, 128.8, 128.0, 127.9, 126.7, 126.3, 126.0, 125.7, 112.5, 99.8, 98.6, 34.9, 32.4, 23.3, 22.7, 22.5, 10.2. Anal. Calcd for $C_{24}H_{22}N_4O$: C, 75.37; H, 5.80; N, 14.65. Found: C, 75.09; H, 5.61; N, 14.89.

*5.3.12. 3-Methyl-4-(thiophen-2-yl)-2,4,6,7,8,9-hexahydropyrazolo[4',3':5,6]pyrano[2,3-b]quinolin-5-amine (**7l**).* Yield 77%; white solid; mp >250 ºC; IR (KBr, cm^{-1}) ν_{max}: 3472 and 3362 (NH_2), 1591 (C=N). ^{1}H NMR (DMSO-d_6, 400 MHz) δ: 11.95 (bs, 1H, NH), 7.22 (dd, 1H, J = 5.2 and J = 1.2 Hz, $H_{5\ thiophen}$), 7.11(dd, 1H, J = 4.8 and J = 1.2 Hz, $H_{3\ thiophen}$), 6.87-6.85 (m, 1H, $H_{3\ thiophen}$), 5.61 (s, 1H, H_4), 5.56 (bs, 2H, NH_2), 2.56 (bs, 2H, $2H_9$), 2.35-2.21 (m, 2H, $2H_6$), 2.10 (s, 3H, CH_3 pyrazol), 1.71 (bs, 4H, $2H_7$ and $2H_8$). ^{13}C NMR (DMSO-d_6, 100 MHz) δ: 155.5, 154.6, 154.0, 150.6, 149.1, 136.4, 126.1, 125.3, 112.8, 99.7, 98.8, 30.4, 29.5, 23.0, 22.3, 10.1. Anal. Calcd for $C_{18}H_{18}N_4OS$: C, 63.88; H, 5.36; N, 16.56. Found: C, 63.61; H, 5.12; N, 16.90.

5.4. In vitro inhibition studies on AChE and BuChE

The inhibitory activities of the target compounds against AChE and BuChE were determined using the spectrophotometric method of Ellman [22]. Five different concentrations of each compound were tested to obtain the range of 20% to 80% enzyme inhibition for AChE and BuChE. The assay solution consisted of 3 ml phosphate buffer (0.1 mol/L^{-1}, pH 8.0), 100 µl of 5,5′-dithio-bis(2-nitrobenzoic acid), 100 µl of 2.5 IU/ml of acetylcholinesterase (AChE, E.C. 3.1.1.7, Type V-S, lyophilized powder, from *electric eel*, 1000 unit) or butyrylcholinesterase (BuChE, E.C. 3.1.1.8, from equine serum) and 100 µl of each test compounds. The mixture was pre-incubated for 10 min followed by the addition of substrate (acetylthiocholine iodide or butyrylthiocholine iodide). Assays were carried out with a blank containing all components except enzyme in order to account the non-enzymatic reaction. Changes in absorbance were measured at 412 nm for 6 min at 25 °C by using an UV Unico Double Beam spectrophotometer.

The IC_{50} values were determined graphically from log concentration vs. % of inhibition curves. All experiments were performed in triplicate.

5.5. Neuroprotection assay against H_2O_2-induced cell death in PC12 cells

Rat differentiated PC12 cells were provided as previously described method [23]. Differentiated PC12 cells were incubated with different concentrations (1, 5 and 10 µM) of the compound for 3 h before treatment with H_2O_2 (300 µM). The occurrence of apoptosis was established after staining with DAPI, and cell viability was measured after 24 h by using the MTT assay. Briefly, 10 µl of MTT solution (5 mg/ml, Sigma) was added to the cell culture media (150 µl) and incubated in a CO_2 incubator for 3.5 h. Thereafter, medium was removed and DMSO (150 µl) was added into the each well and the formazan precipitates were dissolved by shaking the plate for 10 min at speed of 120 rpm. Finally, optical density (OD) was determined at 560 nm on the microplate reader (BioTek synergy HT). Results were adjusted considering OD measured in the blank [24].

5.6. Docking simulations

The program Autodock Vina (AV) 1.1.1 [25] was used for docking simulations. For docking purpose, the crystal structure of *Torpedo californica* acetylcholinesterase (1EVE) was retrieved from Protein Data Bank (http://www.rcsb.org/pdb/home/home.do). To create receptor and ligand structures for docking, the following procedure was conducted. First, the co-crystallized ligand and water molecules were removed from the protein. After that the atomic coordinates of the ligands was prepared using Marvinsketch 5.8.3, 2012, ChemAxon (http://www.chemaxon.com), the 3D structures were constructed using Openbabel 2.3.1 [26]. Then, the receptor and optimized structure of the ligands were converted to required pdbqt format using Autodock Tools 1.5.4 [27]. The Autodock Vina parameters were set as follow; box size: 15×15×15 Å, the center of box: x = 2.023, y = 63.295, z = 67.062 (geometrical center of co-crystallized ligand), the exhaustiveness:100, and the remaining parameters were left unchanged. The calculated geometries were ranked in terms of free energy of binding and the best poses were selected for further analysis. All molecular visualizations were carried out in DS Viewer Pro (Accelrys, Inc., San Diego, CA).

Acknowledgments

This work was supported by a grant from the Research Council of Tehran University of Medical Sciences.

References

[1] A.M. Palmer, Trends Pharmacol. Sci. 32 (2011) 141–147.

[2] R. León, A.G. Garcia, J. Marco-Contelles, Med. Res. Rev. 33 (2013) 139–189.

[3] P. Anand, B. Singh, Arch. Pharm. Res. 36 (2013) 375–399.

[4] N.C. Inestrosa, A. Alvarez, C.A. Pérez, R.D. Moreno, M. Vicente, C. Linker, O.I. Casanueva, C. Soto, J. Garrido, Neuron 16 (1996) 881–891.

[5] M. del Monte-Millán, E. García-Palomero, R. Valenzuela, P. Usán, C. de Austria, P. Muñoz-Ruiz, L. Rubio, I. Dorronsoro, A. Martínez, M. Medina, J. Mol. Neurosci. 30 (2006) 85–88.

[6] A. Gella, N. Durany, Cell Adhesion & Migration 3 (2009) 88–93.

[7] F.M. Longo, S.M. Massa, NeuroRx. 1 (2004) 117–127.

[8] B.J. Sahakian, A.M. Owen, N.J. Morant, S.A. Eagger, S. Boddington, L. Crayton, H.A. Crockford, M. Crooks, K. Hill, R. Levy, Psychopharmacology 110 (1993) 395–401.

[9] P.B. Watkins, H.J. Zimmerman, M.J. Knapp, S.I. Gracon, K.W. Lewis. JAMA 271 (1994) 992–998.

[10] D. Thomae, G. Kirsch, P. Seck, Synthesis (2007) 1027–1032.

[11] D. Thomae, E. Perspicace, S. Hesse, G. Kirsch, P. Seck, Tetrahedron 64 (2008) 9309–9314.

[12] H. Bekolo, G. Kirsch, Can. J. Chem. 85 (2007) 1–6.

[13] D. Thomae, G. Kirsch, P. Seck, Synthesis (2008) 1600–1606.

[14] C.-L. Yang, C.-H. Tseng, Y.-L. Chen, C.-M. Lu, C.-L. Kao, M.-H. Wu, C.-C. Tzeng, Eur. J. Med. Chem. 45 (2010) 602–607.

[15] C. de Los Ríos, J. Egea, J. Marco-Contelles, R. León, A. Samadi, I. Iriepa, I. Moraleda, E. Gálvez, A.G. García, M.G. López, M. Villarroya, A. Romero, J. Med. Chem. 53 (2010) 5129–5143.

[16] D. Silva, M. Chioua, A. Samadi, M. Carmo Carreiras, M.L. Jimeno, E. Mendes, L. Ríos Cde, A. Romero, M. Villarroya, M.G. López, J. Marco-Contelles, J. Eur. J. Med. Chem. 46 (2011) 4676–4681.

[17] E. Maalej, F. Chabchoub, M.J. Oset-Gasque, M. Esquivias-Pérez, M.P. González, L. Monjas, C. Pérez, C. de los Ríos, M.I. Rodríguez-Franco, I. Iriepa, I. Moraleda, M. Chioua, A. Romero, J. Marco-Contelles, A. Samadi, Eur. J. Med. Chem. 54 (2012) 750–763.

[18] E. Maalej, F. Chabchoub, A. Samadi, C. De los Rios, A. Perona, A. Morreale, J. Marco-Contelles, Bioorg. Med. Chem. Lett. 21 (2011) 2384–2388.

[19] [a] H. Nadri, M. Pirali-Hamedani, M. Shekarchi, M. Abdollahi, V. Sheibani, M. Amanlou, A. Shafiee, A. Foroumadi, Bioorg. Med. Chem. 18 (2010) 6360–6366.

[b] M. Alipour, M. Khoobi, A. Foroumadi, H. Nadri, A. Moradi, A. Sakhteman, et al. Bioorg. Med. Chem. 20 (2012) 7214–7222.

[c] M. Alipour, M. Khoobi, H. Nadri, A. Sakhteman, A. Moradi, M. Ghandi, et al. Arch. Pharm. Chem. Life Sci. 346 (2013) 577–587.

[d] S.F. Razavi, M. Khoobi, H. Nadri, A. Sakhteman, et al. Eur. J. Med. Chem. 64 (2013) 252–259.

[e] M. Khoobi, M. Alipour, A. Moradi, A. Sakhteman, H. Nadri, et al. Eur. J. Med. Chem. 68 (2013) 291–300.

[f] M. Khoobi, M. Alipour, A. Sakhteman, H. Nadri, A. Moradi, et al. Eur. J. Med. Chem. 68 (2013) 260–269.

[g] H. Akrami, B.F. Mirjalili, M. Khoobi, H. Nadri, A. Moradi, et al. Eur. J. Med. Chem. Available online 19 January 2014, http://dx.doi.org/10.1016/j.ejmech.2014.01.017

[20] H. Mecadon, M.R. Rohman, I. Kharbangar, B.M. Laloo, I. Kharkongor, M. Rajbangshi, B. Myrboh, Tetrahedron Lett. 52 (2011) 3228–3231.

[21] M. Khoobi, M. Alipour, A. Moradi, A. Sakhteman, H. Nadri, S.F. Razavi, M. Ghandi, A. Foroumadi, A. Shafiee, Eur. J. Med. Chem. 68 (2013) 291–300.

[22] G.L. Ellman, K.D. Courtney, V. Andres, R.M. Featherstone, Biochem. Pharmacol. 7 (1961) 88–95.

[23] S.H. Koh, S.H. Kim, H. Kwon, Y. Park, K.S. Kim, C.W. Song, J. Kim, M.H. Kim, H.J. Yu, J.S. Henkel, H.K. Jung, Brain Res. Mol. Brain Res. 118 (2003) 72–81.

[24] D. Zsolt, A. Juhász, M. Gálfi, K. Soós, R. Papp, D. Zádori, B. Penke, Brain Res. Bull. 62 (2003) 223–229.

[25] O. Trott, A.J. Olson, J. Comput. Chem. 31 (2010) 455–461.

[26] N.M. O'Boyle, M. Banck, C.A. James, C. Morley, T. Vandermeersch, G.R. Hutchison, J. Cheminform 3 (2011) 33.

[27] M.F. Sanner, A programming language for software integration and development, J. Mol. Graph. Model. 17 (1999) 57–61.

Captions:

Fig. 1. The structures of tacrine and some previously reported tacrine-based anti-AChE agents (**A**, **B** and **C**). Compounds **7a-l** were designed in this work, as new tetracyclic tacrine analogs containing pyrano[2,3-*c*]pyrazole.

Fig. 2. Inhibition kinetics of compound **7h** using Lineweaver-Burk plot with *eel*AChE.

Fig. 3. The Lineweaver-Burk secondary plot of compound **7h**, slope vs. various concentrations of compound **7h**.

Fig. 4. Neuroprotective effect of compound **7h** against H_2O_2-induced cell death in PC12 cells. Data are expressed as mean ± SD (n = 8), $^{###}$ P <0.001 vs. control, *** P <0.001 vs. H_2O_2 and ** P <0.05 vs. H_2O_2 treated only.

Fig. 5. The proposed orientation of *R* (green) and *S* (magenta) enantiomers of **7h** in the AChE active site.

Fig. 6. Illustration of (*R*)-**7h** binding mode in the AChE active site. The hydrogen bond is presented as red dashed line and rings having π–π stacking are filled with yellow color.

Fig. 7. Illustration of (*S*)-**7h** enantiomer binding mode in the AChE active site. The hydrogen bond is presented as red dashed line and rings having π–π stacking are filled with green color.

Scheme 1. Synthesis of compounds **7a-l**.

Table 1

Inhibitory activity of the target compounds **7a-l** against AChE and BuChE

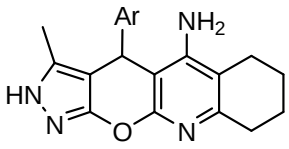

Compound	Ar	IC_{50} (μM)[a] AChE	IC_{50} (μM) BuChE
7a	4-Tolyl	0.75 ± 0.04	4.5 ± 0.2
7b	2-Fluorophenyl	0.59 ± 0.04	33.0 ± 2.1
7c	4- Fluorophenyl	0.81 ± 0.05	25.0 ± 1.8
7d	3-Nitrophenyl	3.27 ± 0.19	>100
7e	4-Methoxyphenyl	0.31 ± 0.02	>100
7f	2-Methoxyphenyl	>10	>100
7g	2,5-Dimethoxyphenyl	0.50 ± 0.03	>100
7h	3,4-Dimethoxyphenyl	0.19 ± 0.01	>100
7i	3,4,5-Trimethoxyphenyl	2.18 ± 0.13	>100
7j	2,3-Dichlorophenyl	0.87 ± 0.06	>100
7k	1-Naphthyl	0.32 ± 0.02	15.0 ± 1.1
7l	2-Thienyl	0.72 ± 0.04	16.0 ± 1.1
Tacrine	-	0.28 ± 0.02	0.35 ± 0.2

[a] Data are expressed as mean ± S.E. of at least three different experiments.

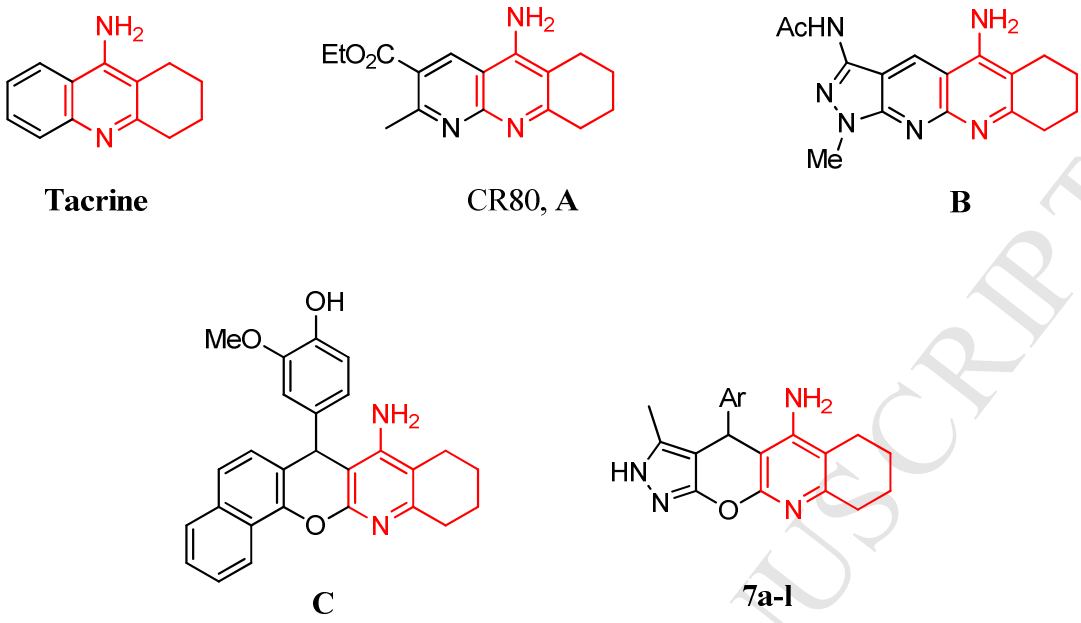

Fig. 1. The structures of tacrine and some previously reported tacrine-based anti-AChE agents (**A**, **B** and **C**). Compounds **7a-l** were designed in this work, as new tetracyclic tacrine analogs containing pyrano[2,3-*c*]pyrazole.

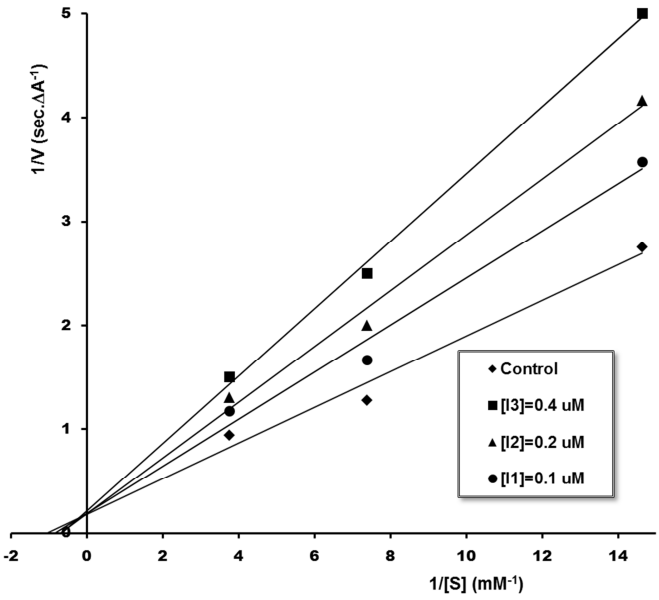

Fig. 2. Inhibition kinetics of compound **7h** using Lineweaver-Burk plot with *eel*AChE.

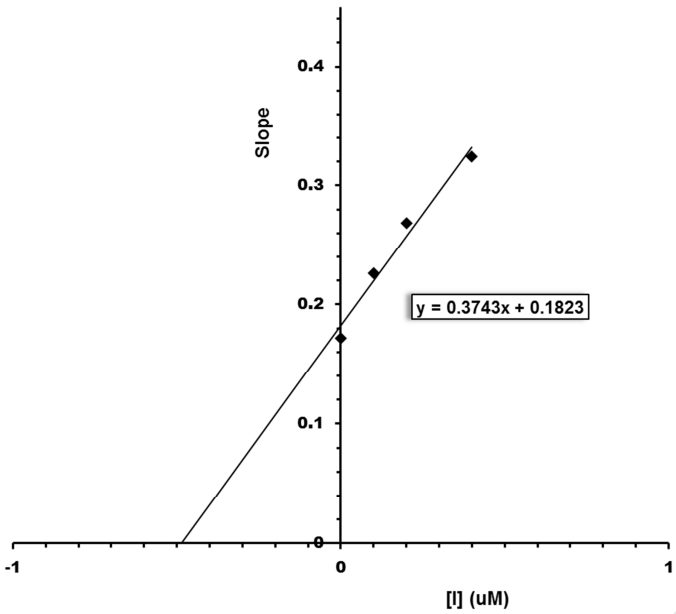

Fig. 3. The Lineweaver-Burk secondary plot of compound **7h**, slope vs. various concentrations of compound **7h**.

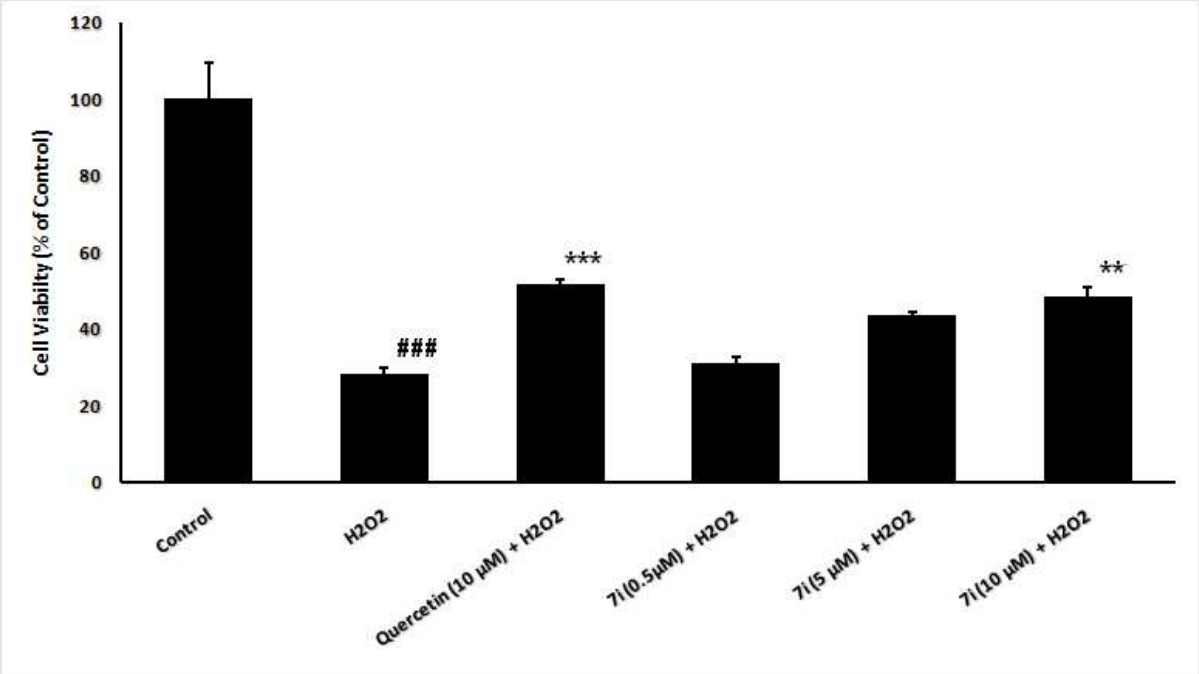

Fig. 4. Neuroprotective effect of compound **7h** against H_2O_2-induced cell death in PC12 cells. Data are expressed as mean ± SD (n = 8), $^{###}$ P <0.001 vs. control, *** P <0.001 vs. H_2O_2 and **P <0.05 vs. H_2O_2 treated only.

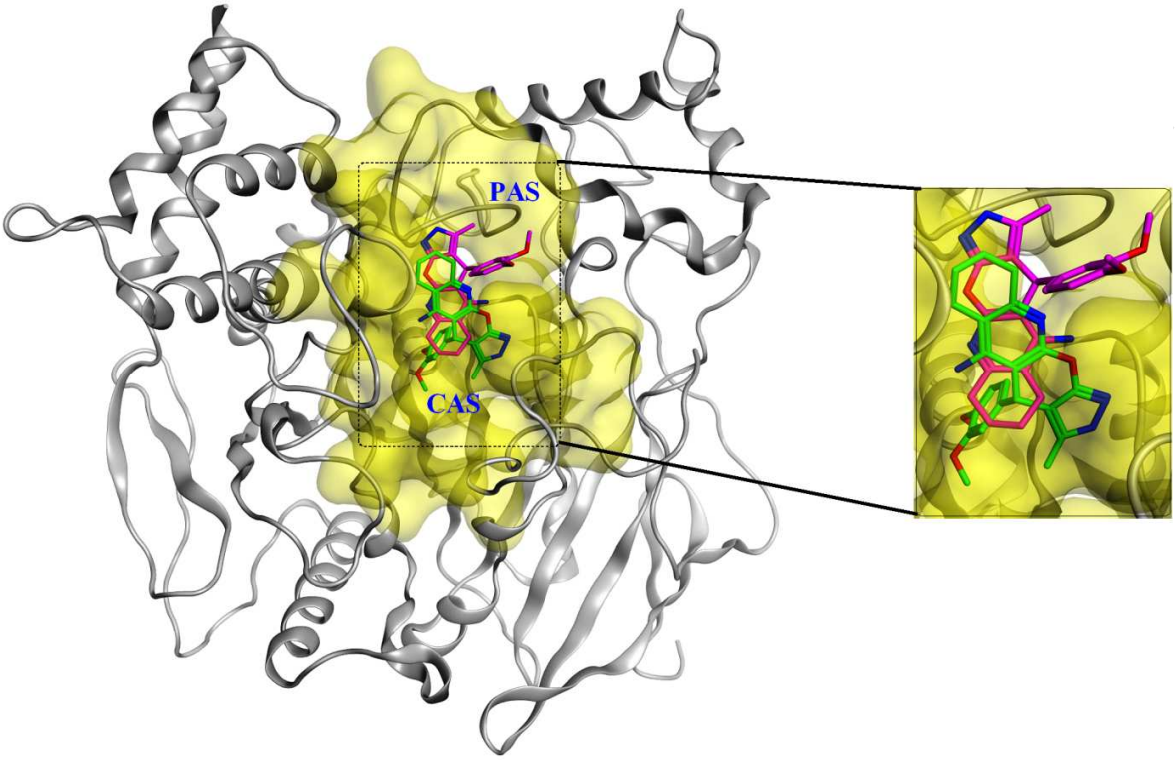

Fig. 5. The proposed orientation of *R* (green) and *S* (magenta) enantiomers of **7h** in the AChE active site.

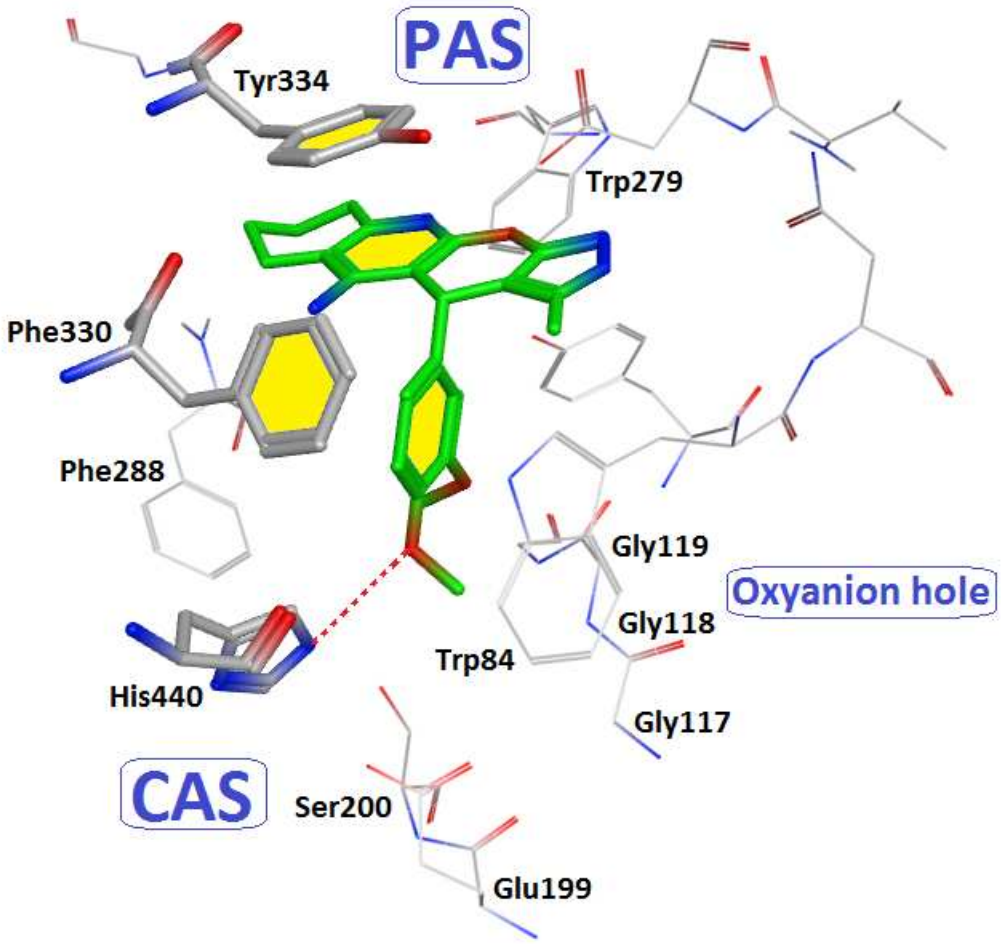

Fig. 6. Illustration of (*R*)-**7h** binding mode in the AChE active site. The hydrogen bond is presented as red dashed line and rings having π–π stacking are filled with yellow color.

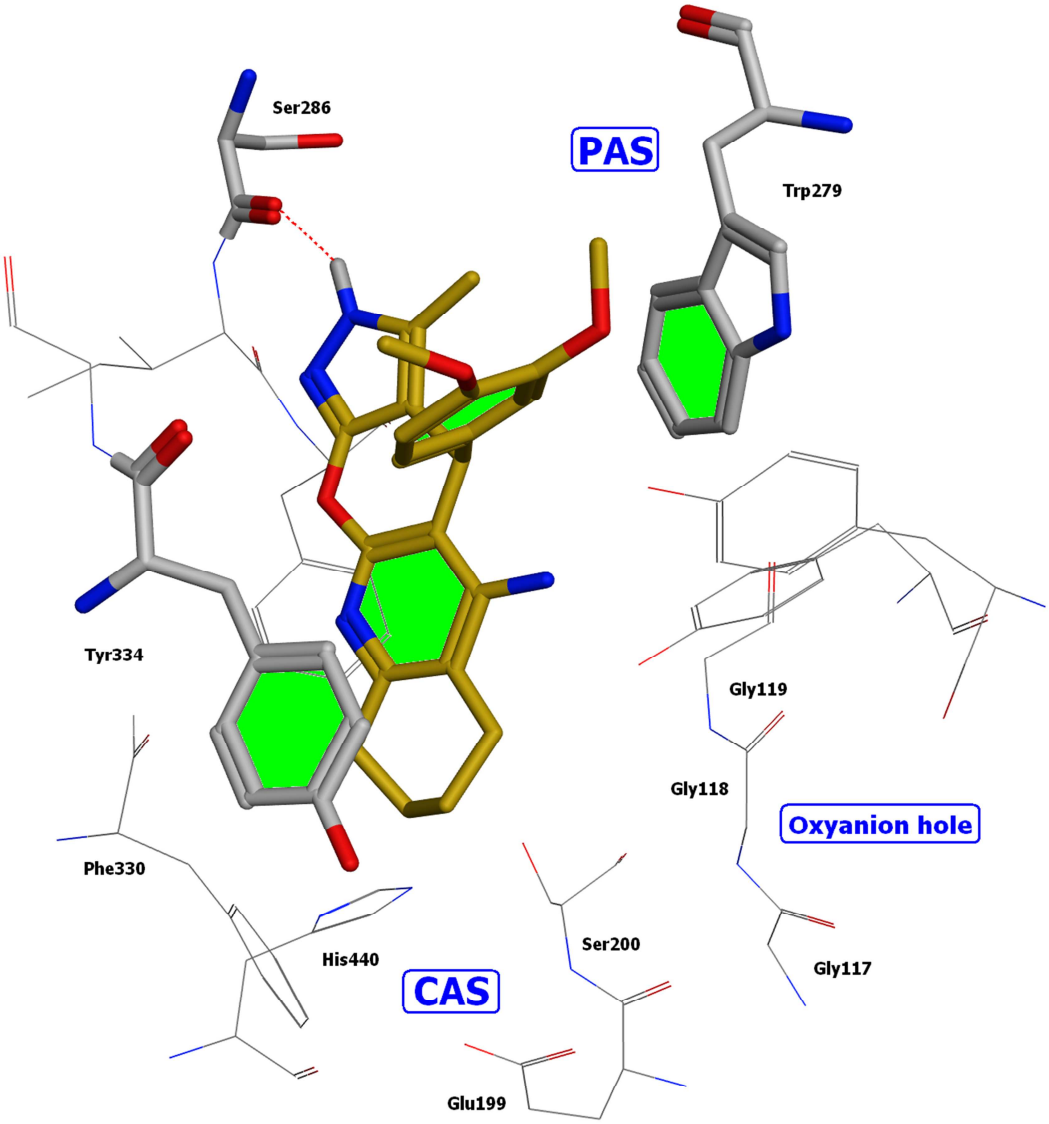
Ser286
PAS
Trp279
Tyr334
Gly119
Gly118
Oxyanion hole
Phe330
His440
CAS
Ser200
Gly117
Glu199

Fig. 7. Illustration of (*S*)-**7h** enantiomer binding mode in the AChE active site. The hydrogen bond is presented as red dashed line and rings having π–π stacking are filled with green color.

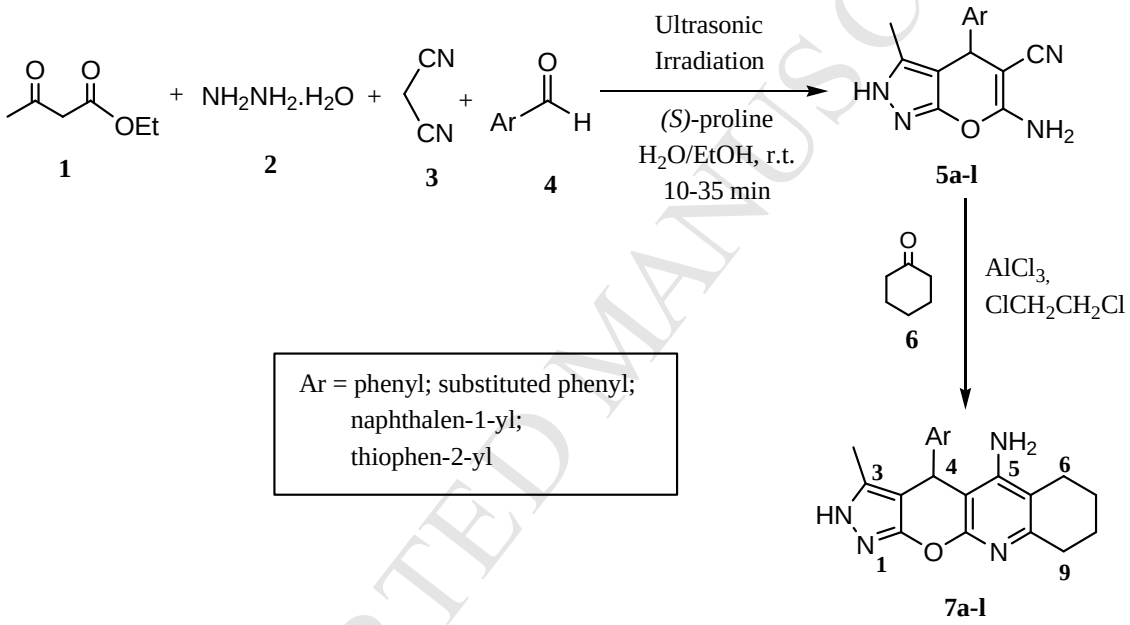

Scheme 1. Synthesis of compounds **7a-l**.

Highlights

- A series of tacrine-based compounds **7a-l** were synthesized as AChE inhibitors.
- Compound **7h** bearing a 3,4-dimethoxyphenyl group was the most active derivative.
- Compound **7h** with IC_{50} = 0.19 µM was more potent than reference drug tacrine.
- Compound **7h** could significantly protect neurons against oxidative stress.
- Docking study showed that (*R*)-**7h** preferably binds to CAS while (*S*)-**7h** binds to PAS.

Supplementary material

New tetracyclic tacrine analogs containing pyrano[2,3-c]pyrazole: efficient synthesis, biological assessment and docking simulation study

Mehdi Khoobi, Farzaneh Ghanoni, Hamid Nadri, Alireza Moradi, Morteza Pirali Hamedani, Farshad Homayouni Moghadam, Saeed Emami, Mohsen Vosooghi[a], Reza Zadmard, Alireza Foroumadi, Abbas Shafiee*

^{1}H and ^{13}C spectra for selected compounds:

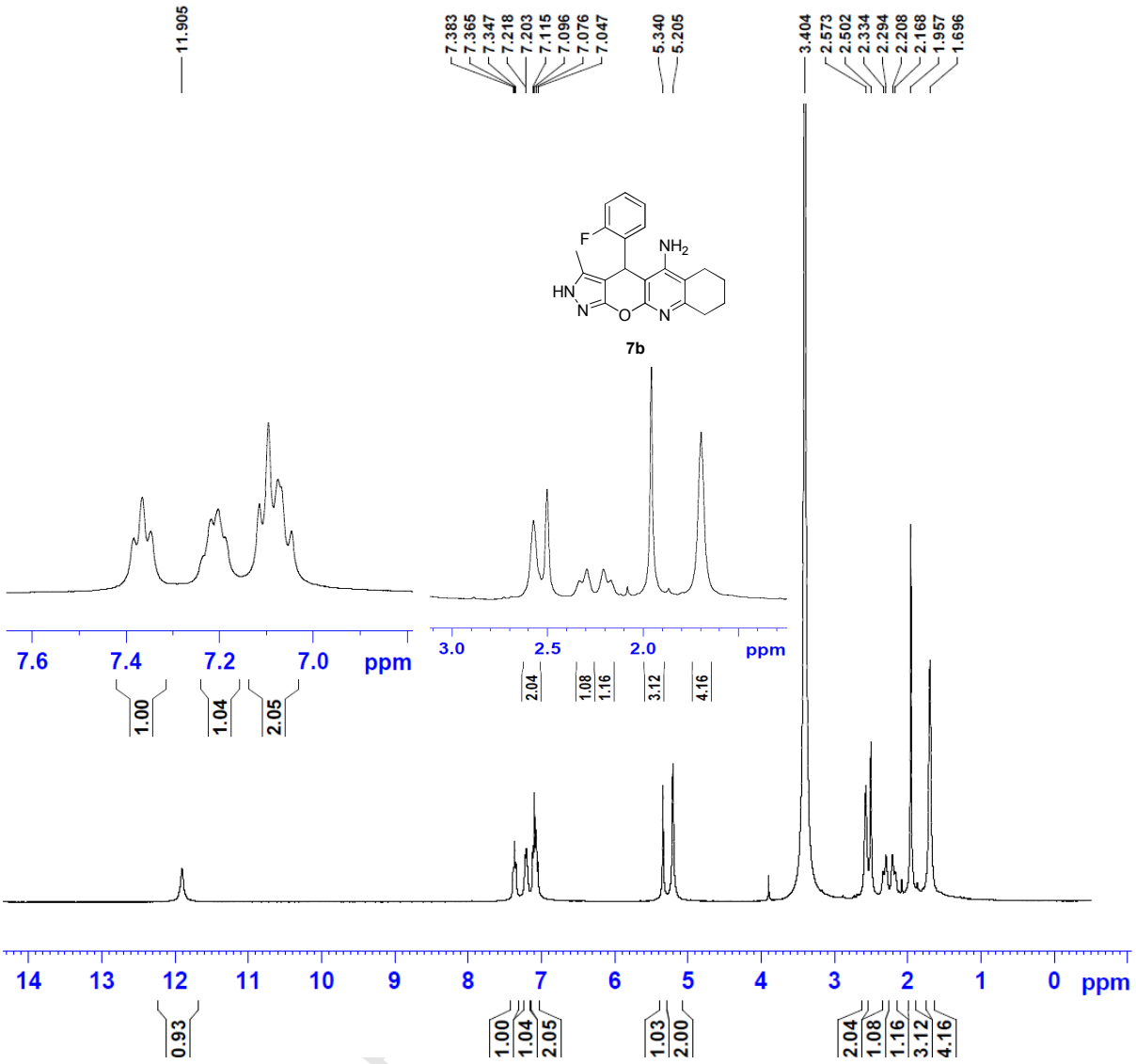
11.905
7.383
7.365
7.347
7.218
7.203
7.115
7.096
7.076
7.047
5.340
5.205
3.404
2.573
2.502
2.334
2.294
2.208
2.168
1.957
1.696
F
NH2
HN
N
O
N
7b
7.6
7.4
7.2
7.0
ppm
1.00
1.04
2.05
3.0
2.5
2.0
ppm
2.04
1.08
1.16
3.12
4.16
14
13
12
11
10
9
8
7
6
5
4
3
2
1
0
ppm
0.93
1.00
1.04
2.05
1.03
2.00
2.04
1.08
1.16
3.12
4.16

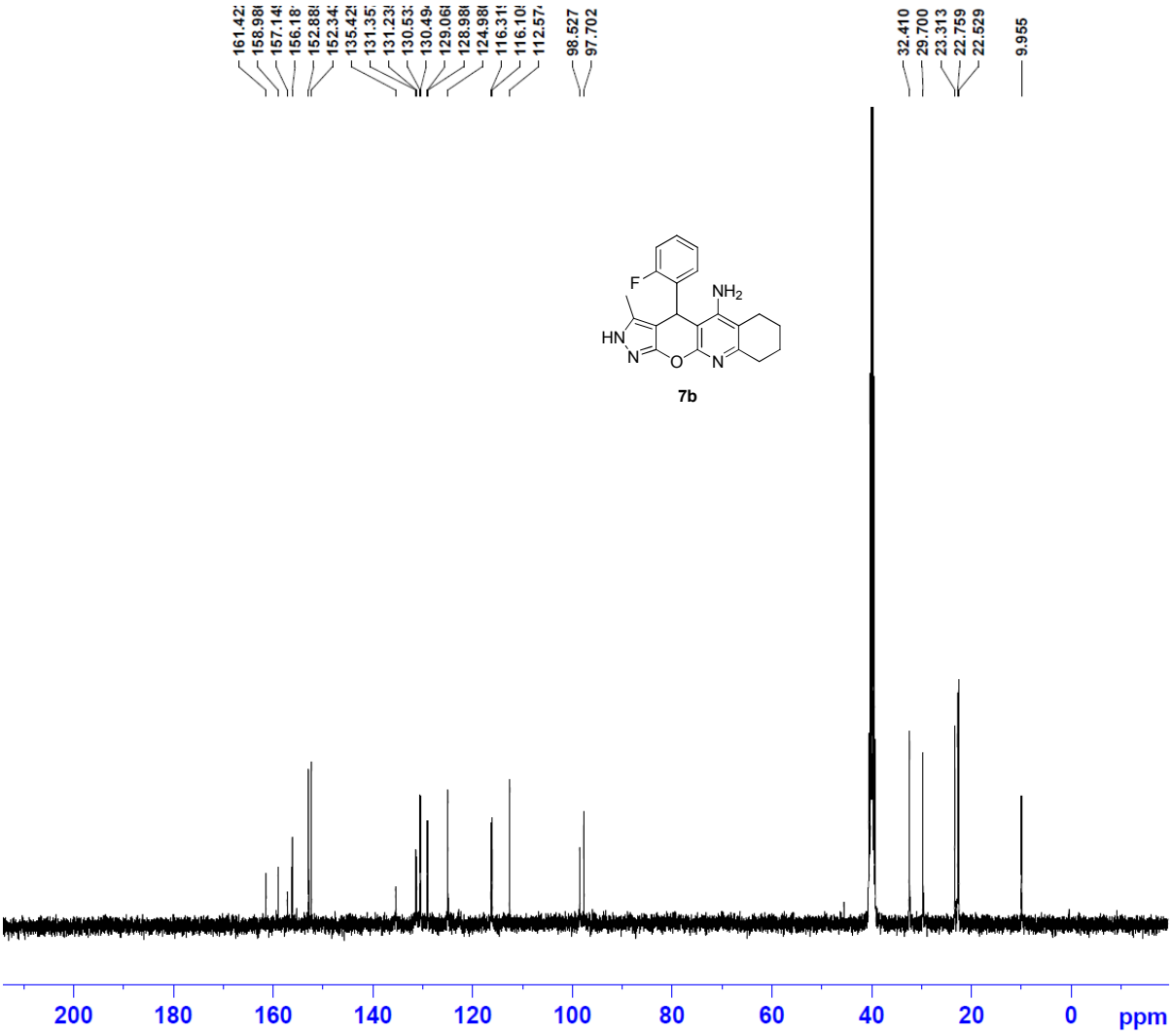

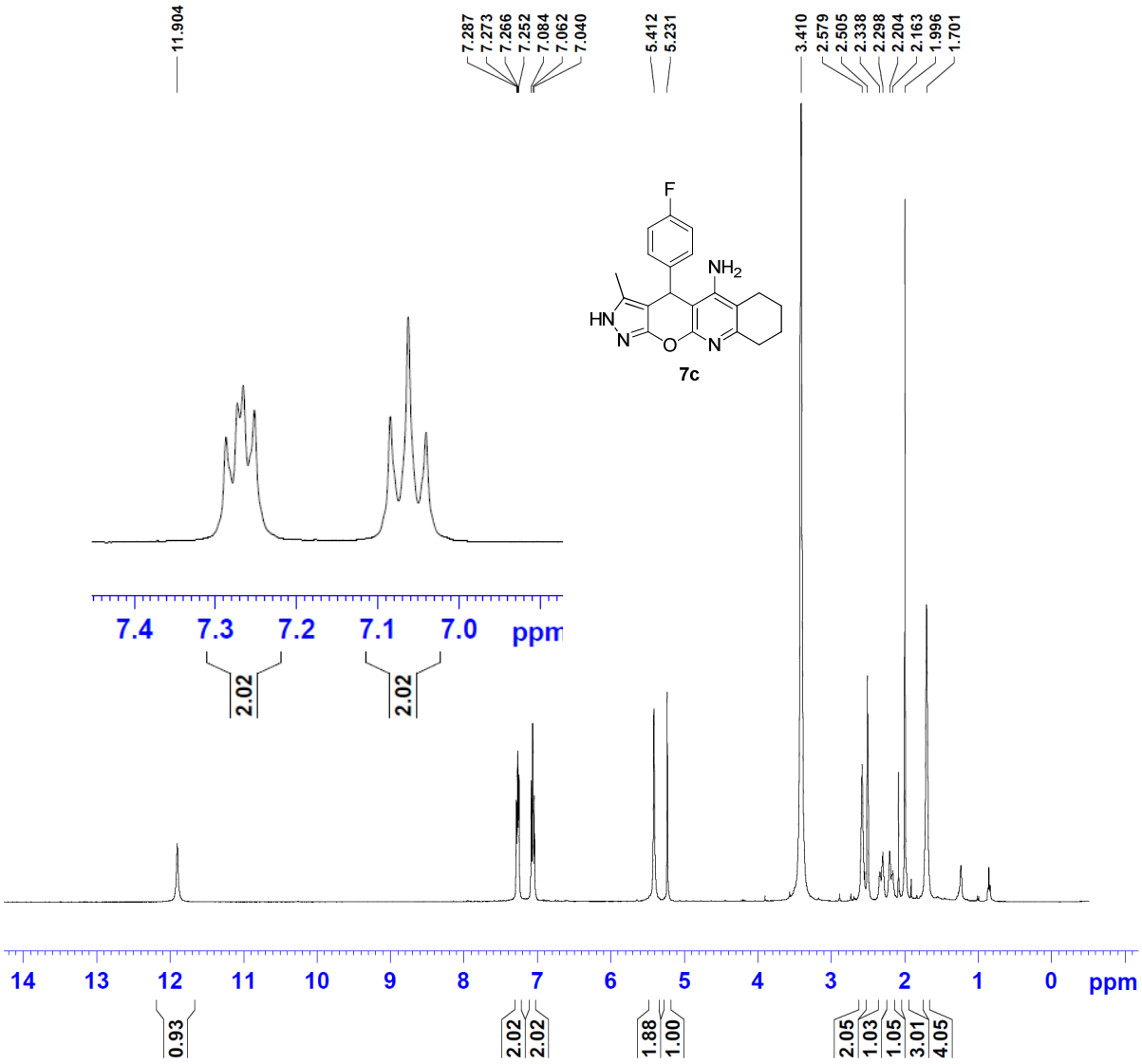
11.904
7.287
7.273
7.266
7.252
7.084
7.062
7.040
5.412
5.231
3.410
2.579
2.505
2.338
2.298
2.204
2.163
1.996
1.701
F
NH2
HN
N
O
N
7c
7.4
7.3
7.2
7.1
7.0
ppm
2.02
2.02
14
13
12
11
10
9
8
7
6
5
4
3
2
1
0
ppm
0.93
2.02
2.02
1.88
1.00
2.05
1.03
1.05
3.01
4.05

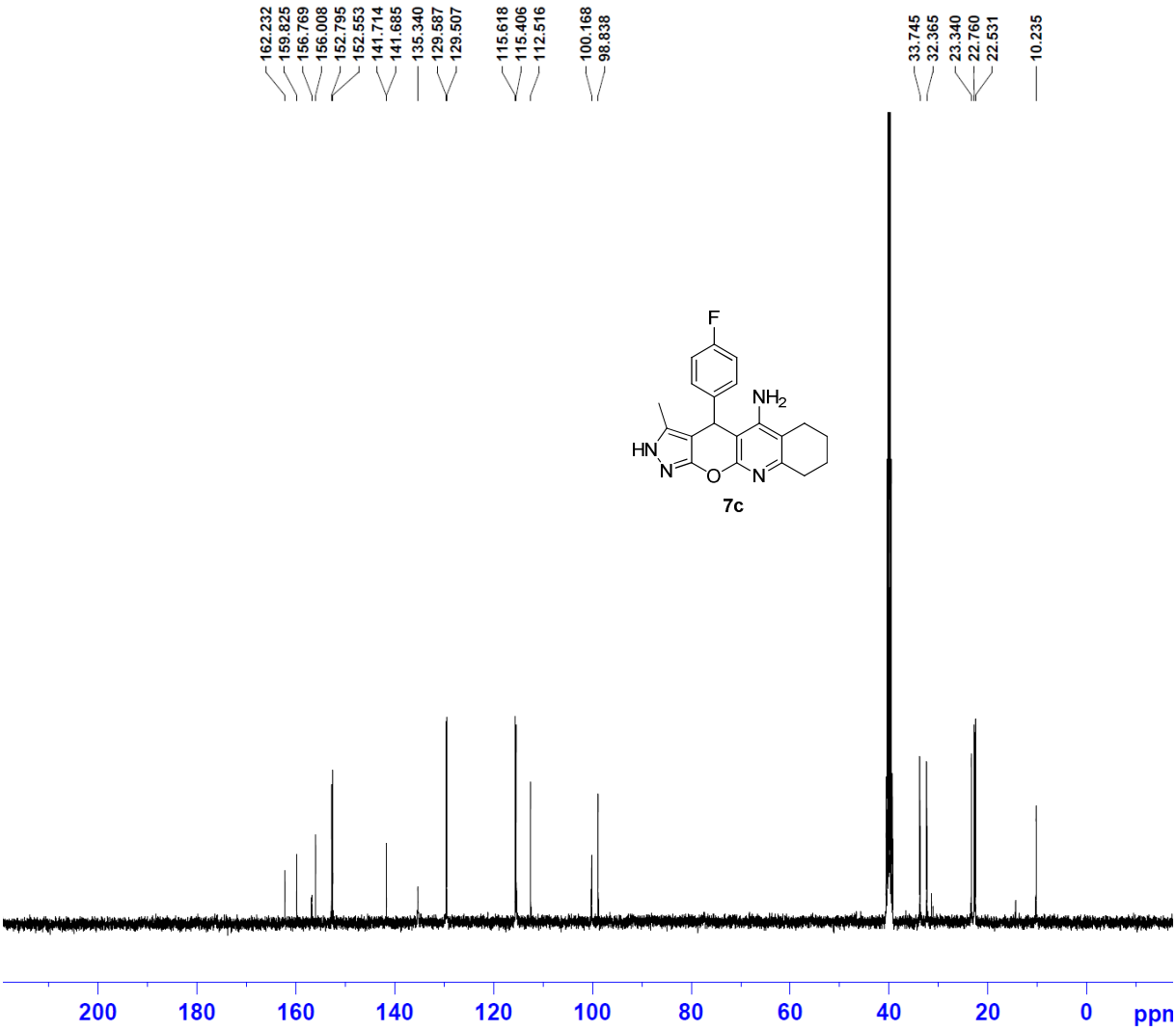
162.232
159.825
156.769
156.008
152.795
152.553
141.714
141.685
135.340
129.587
129.507
115.618
115.406
112.516
100.168
98.838
33.745
32.365
23.340
22.760
22.531
10.235
F
NH2
HN
N
O
N
7c
200
180
160
140
120
100
80
60
40
20
0
ppn

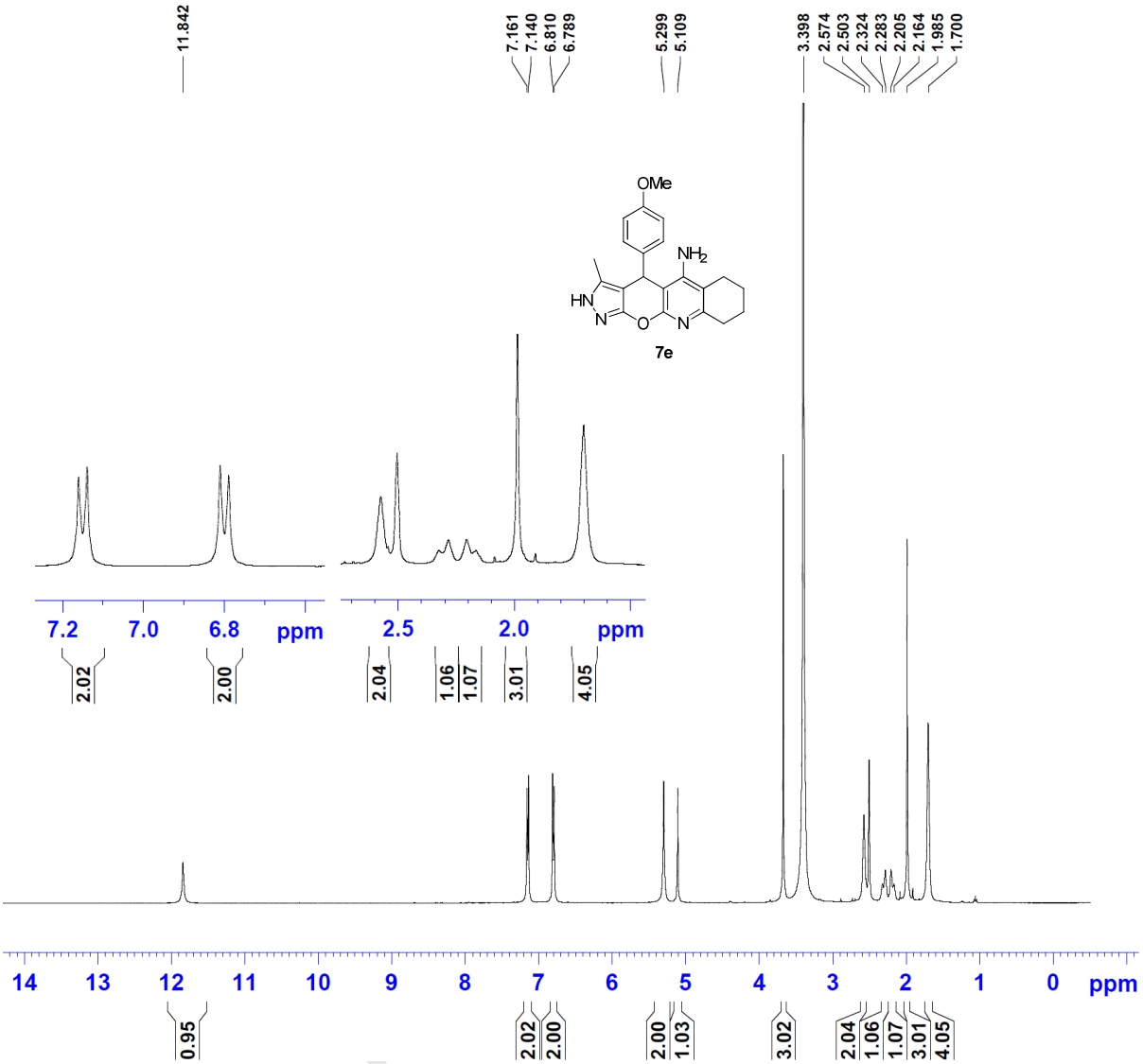
11.842
7.161
7.140
6.810
6.789
5.299
5.109
3.398
2.574
2.503
2.324
2.283
2.205
2.164
1.985
1.700
OMe
NH2
HN
N
O
N
7e
7.2
7.0
6.8
ppm
2.5
2.0
ppm
2.02
2.00
2.04
1.06
1.07
3.01
4.05
14
13
12
11
10
9
8
7
6
5
4
3
2
1
0
ppm
0.95
2.02
2.00
2.00
1.03
3.02
2.04
1.06
1.07
3.01
4.05

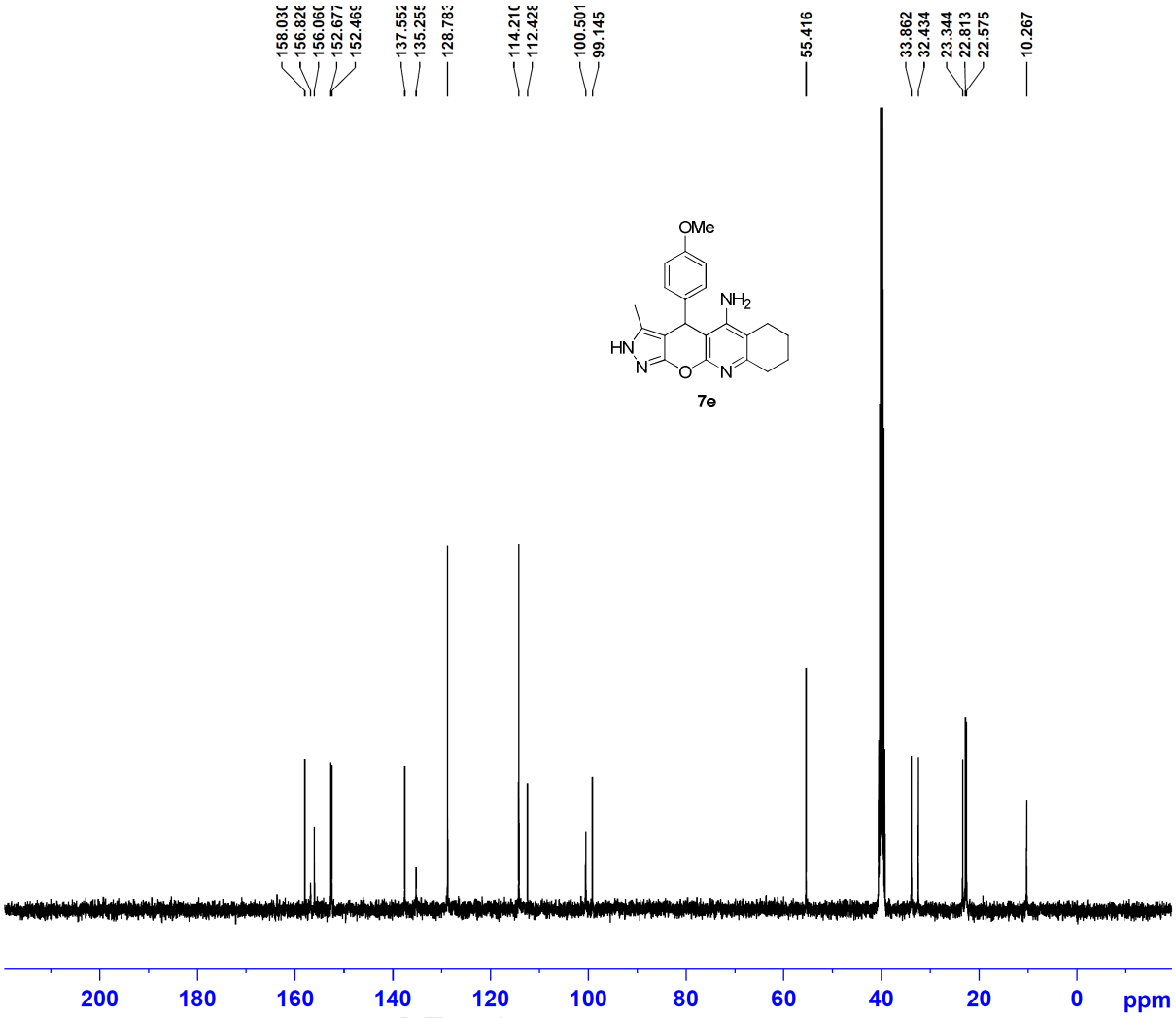
158.03
156.82
156.06
152.67
152.46
137.55
135.25
128.78
114.21
112.42
100.50
99.145
55.416
33.862
32.434
23.344
22.813
22.575
10.267
OMe
NH2
HN
N
O
N
7e
200
180
160
140
120
100
80
60
40
20
0
ppm

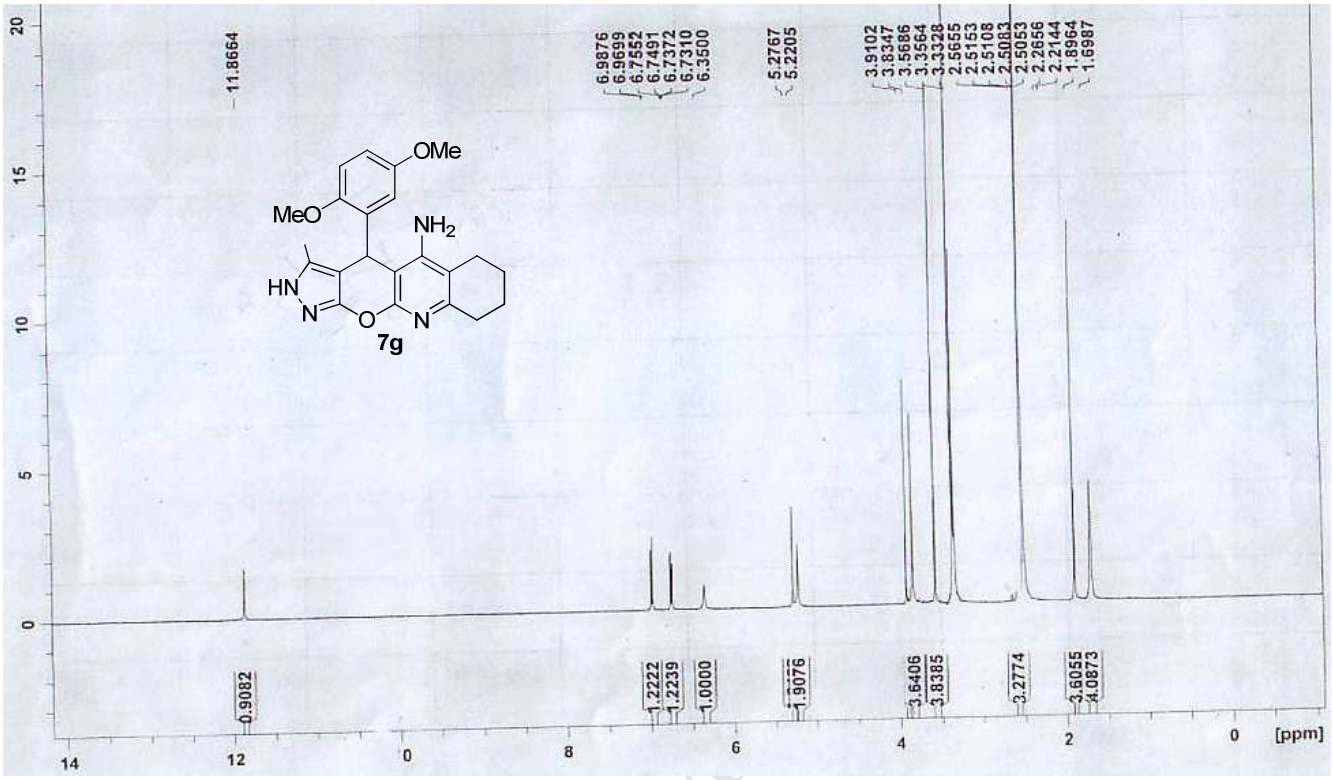

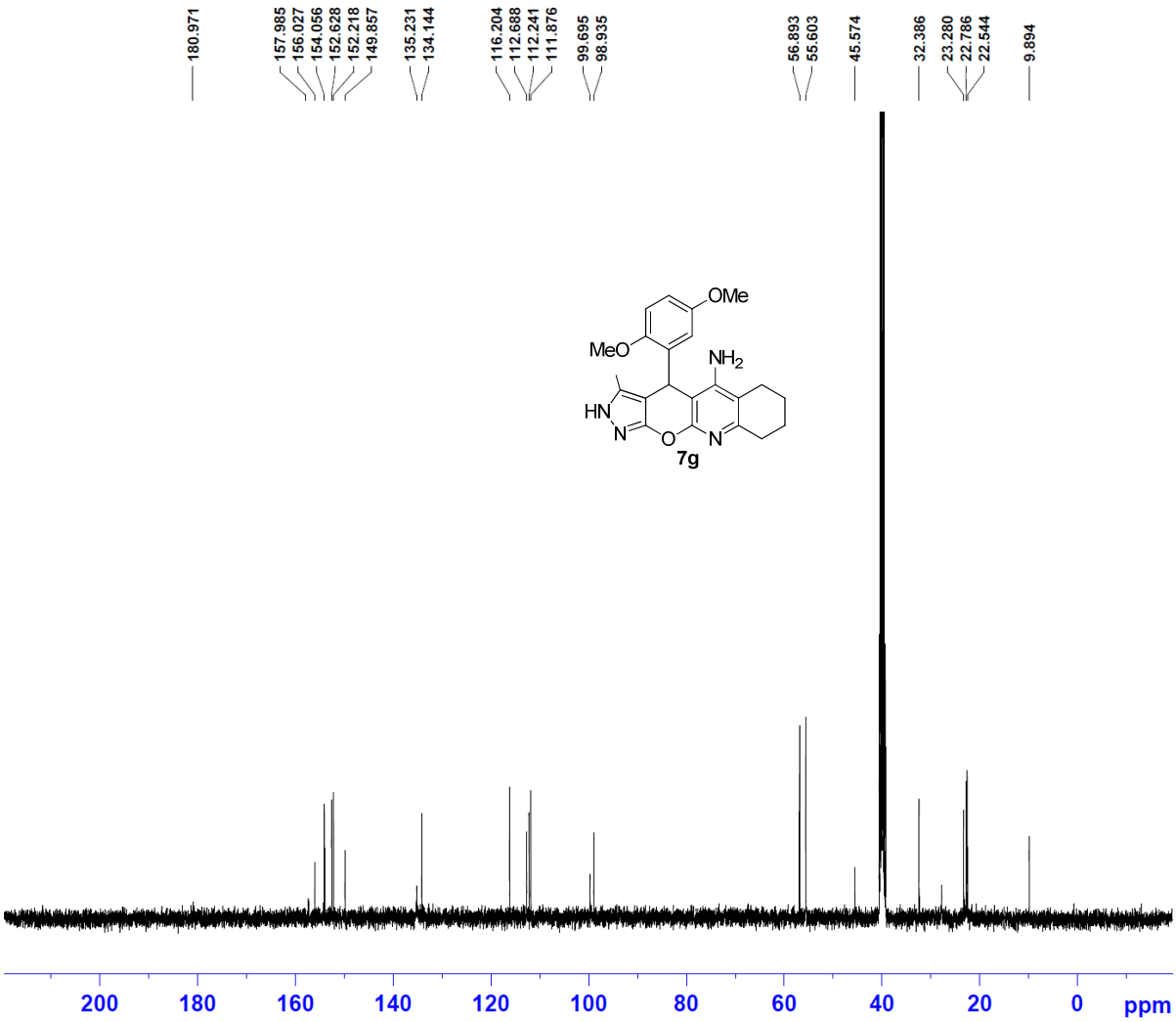

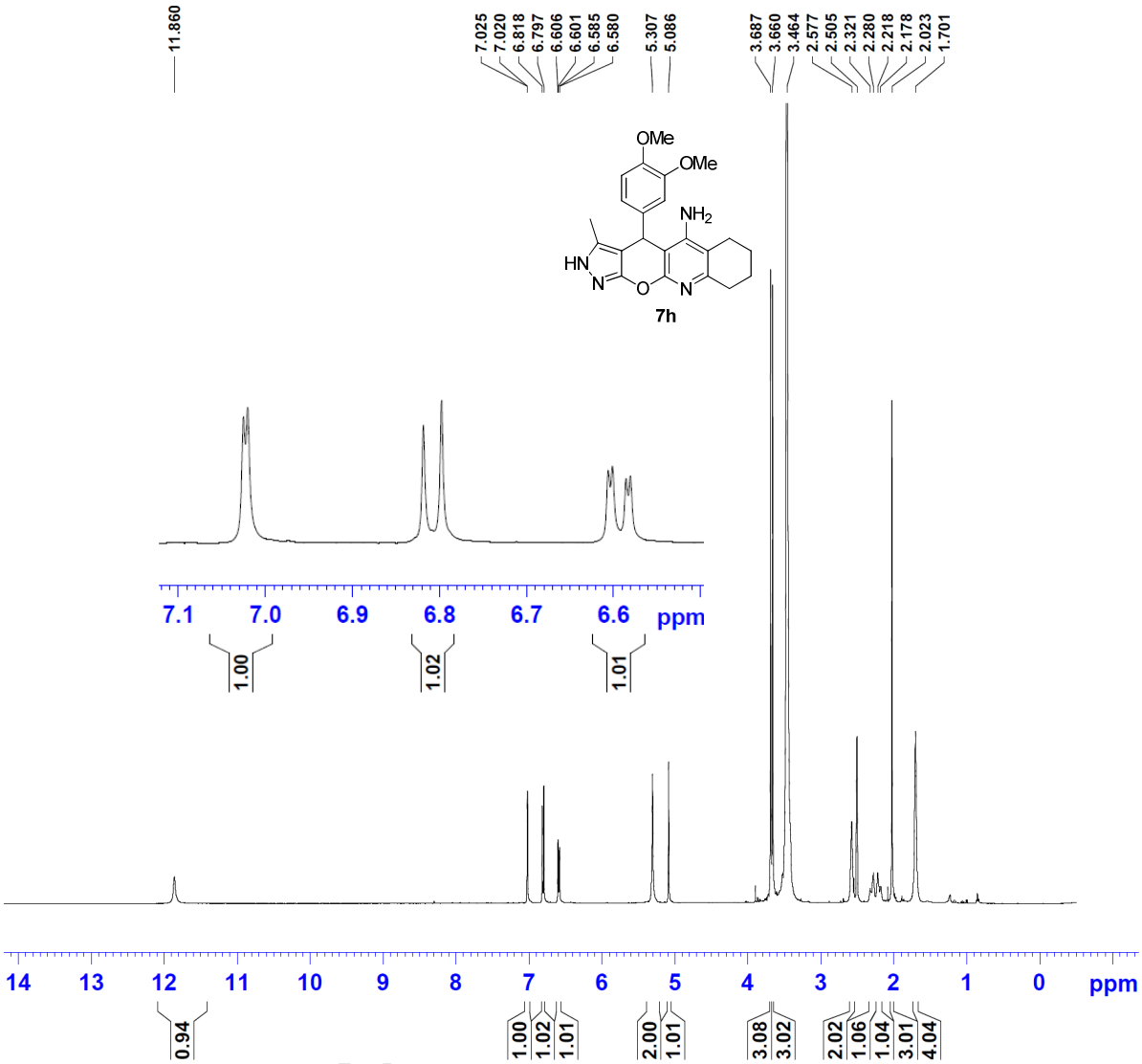
11.860
7.025
7.020
6.818
6.797
6.606
6.601
6.585
6.580
5.307
5.086
3.687
3.660
3.464
2.577
2.505
2.321
2.280
2.218
2.178
2.023
1.701
OMe
OMe
NH2
HN
N
O
N
7h
7.1
7.0
6.9
6.8
6.7
6.6
ppm
1.00
1.02
1.01
14
13
12
11
10
9
8
7
6
5
4
3
2
1
0
ppm
0.94
1.00
1.02
1.01
2.00
1.01
3.08
3.02
2.02
1.06
1.04
3.01
4.04

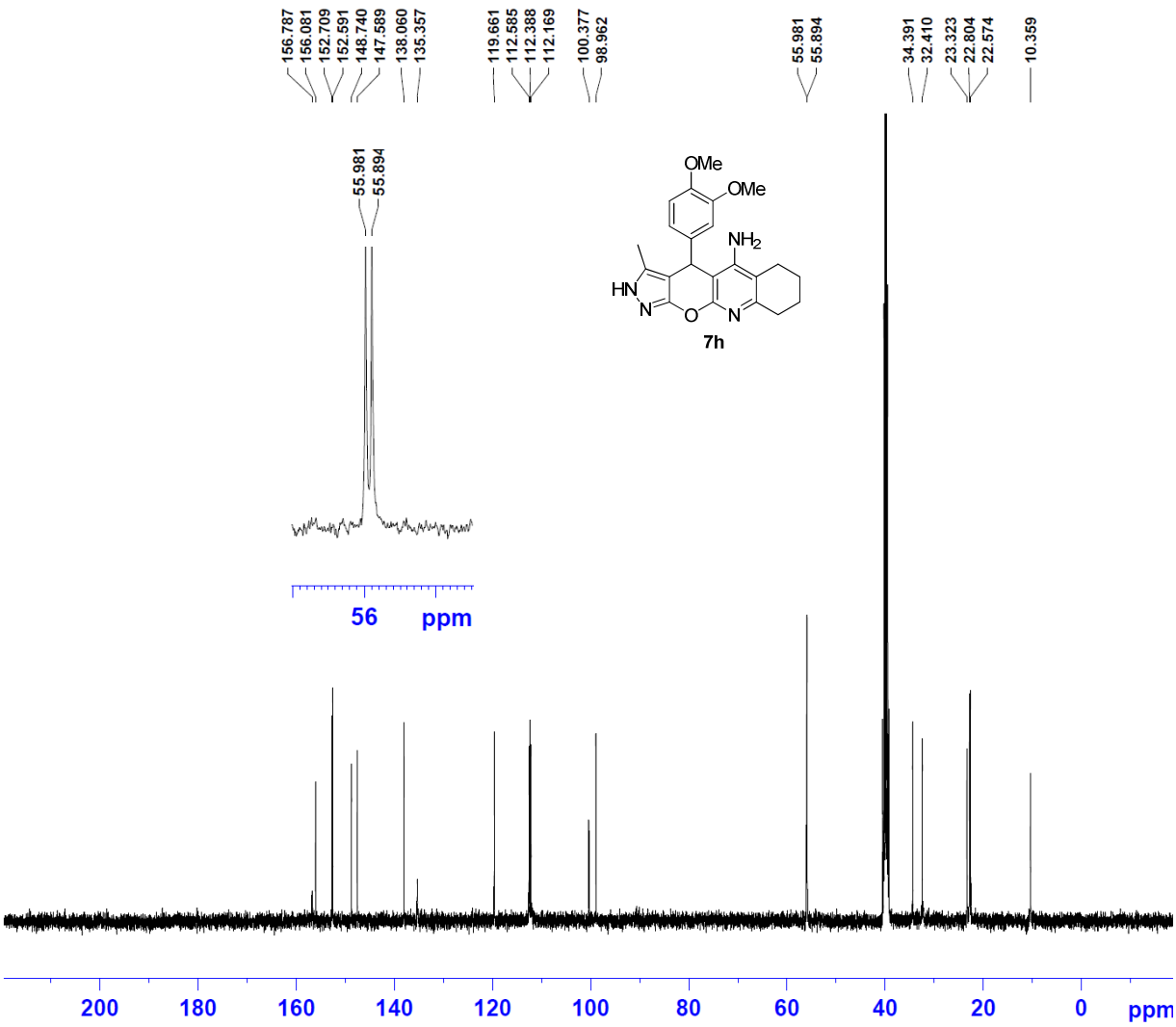

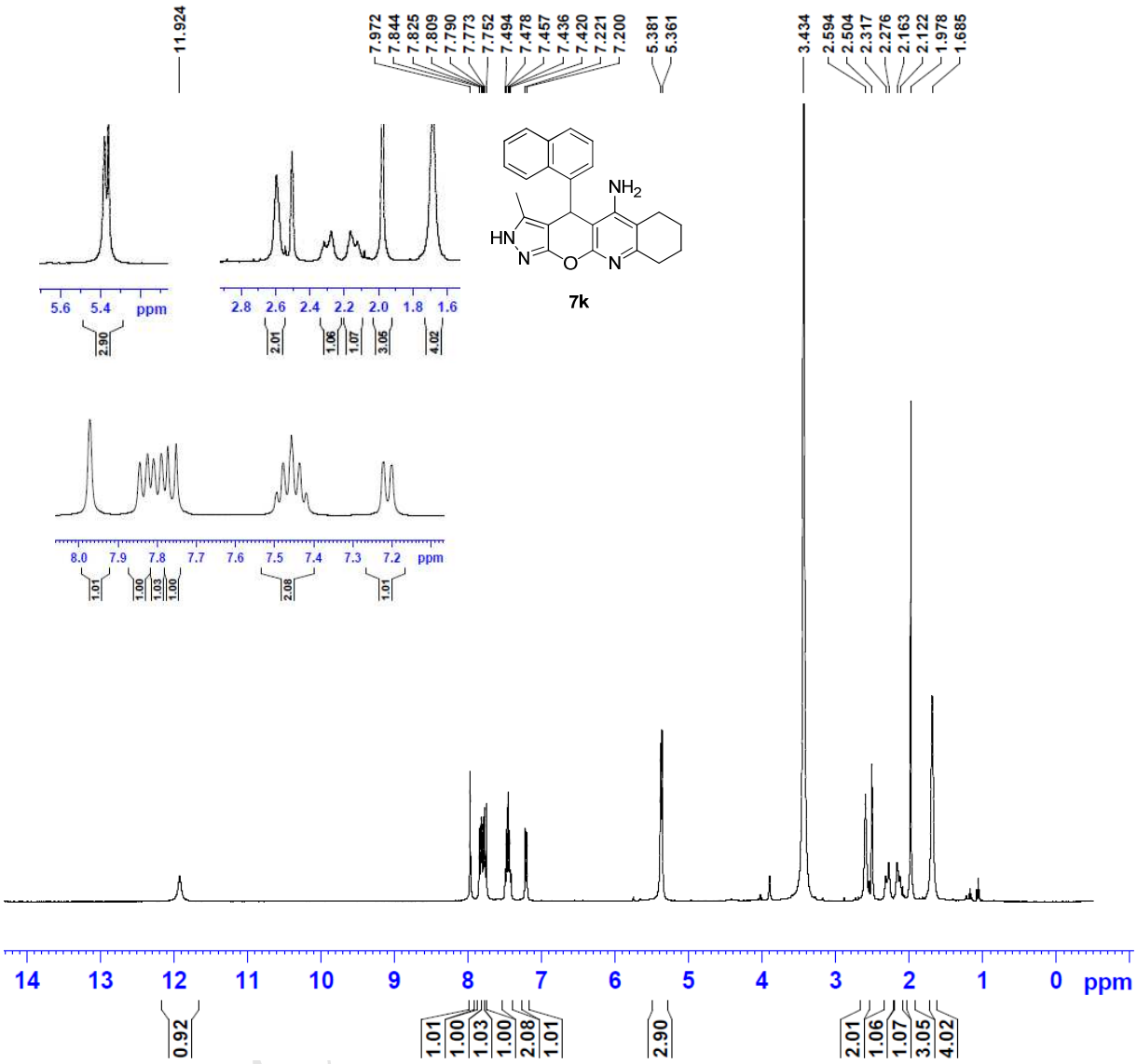
11.924
7.972
7.844
7.825
7.809
7.790
7.773
7.752
7.494
7.478
7.457
7.436
7.420
7.221
7.200
5.381
5.361
3.434
2.594
2.504
2.317
2.276
2.163
2.122
1.978
1.685
NH2
HN
N
O
N
7k
ppm
0.92
1.01
1.00
1.03
1.00
2.08
1.01
2.90
2.01
1.06
1.07
3.05
4.02

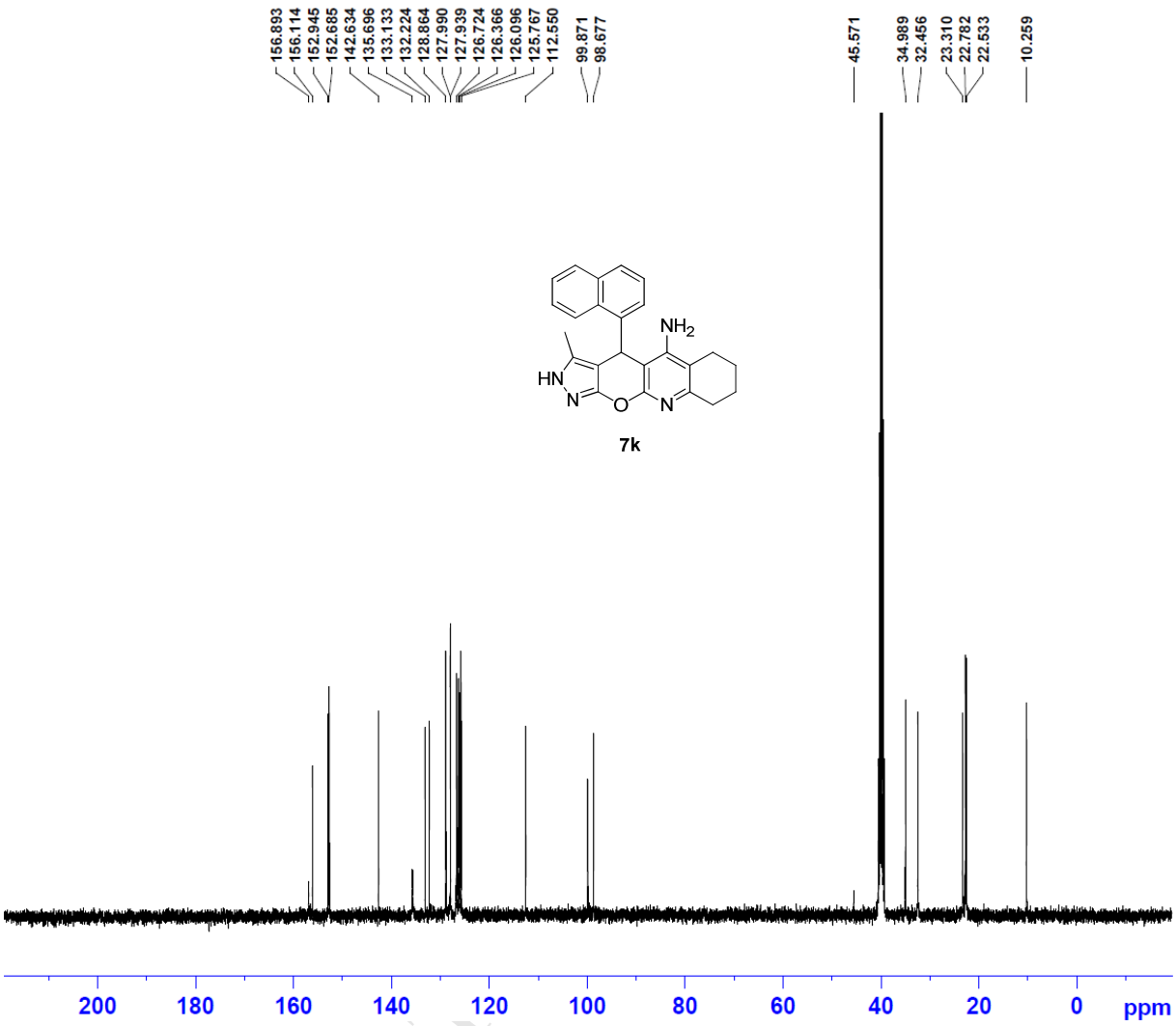

7k

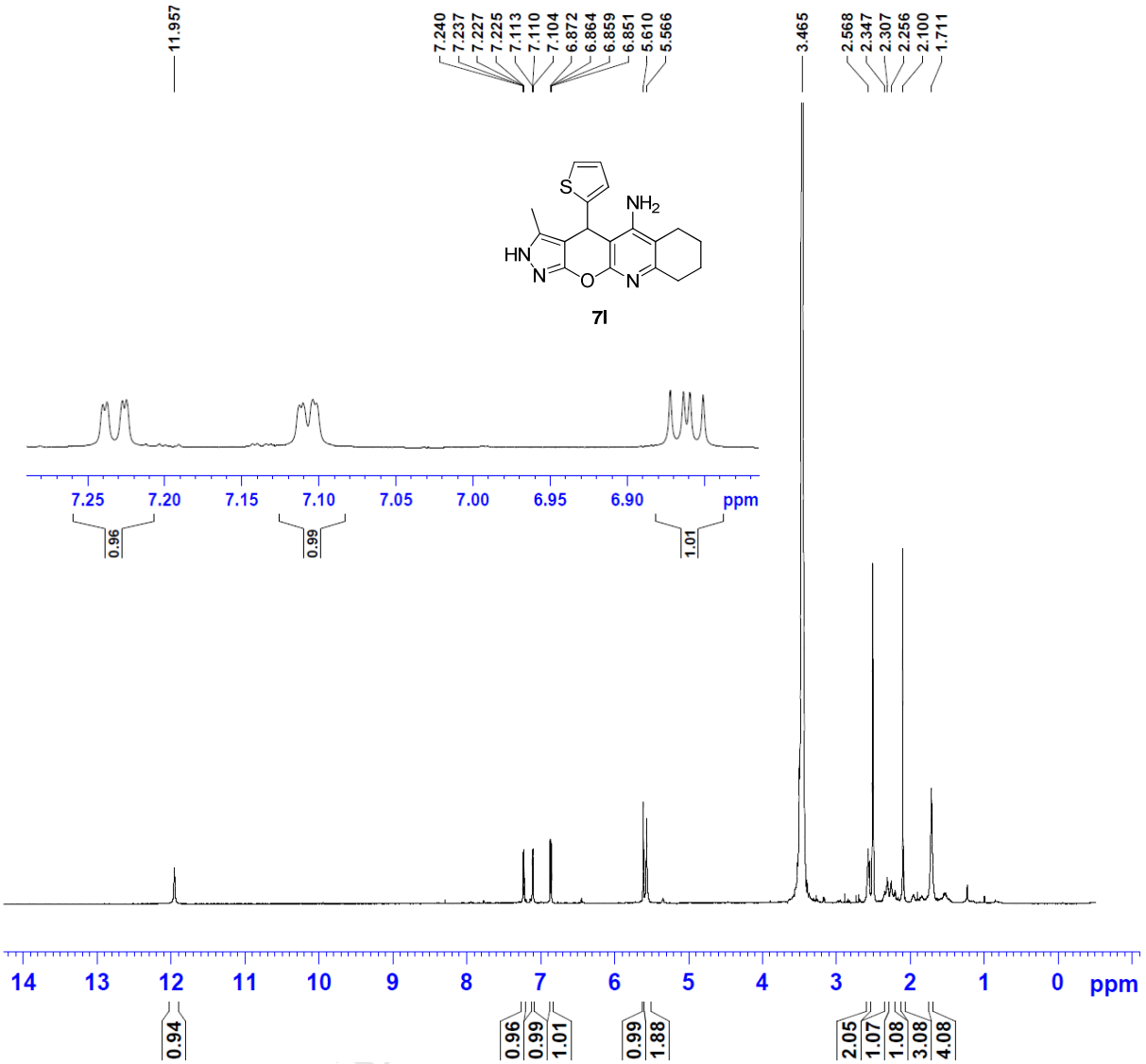
11.957
7.240
7.237
7.227
7.225
7.113
7.110
7.104
6.872
6.864
6.859
6.851
5.610
5.566
3.465
2.568
2.347
2.307
2.256
2.100
1.711
S
NH2
HN
N
O
N
7.25
7.20
7.15
7.10
7.05
7.00
6.95
6.90
ppm
0.96
0.99
1.01
14
13
12
11
10
9
8
7
6
5
4
3
2
1
0
ppm
0.94
0.96
0.99
1.01
0.99
1.88
2.05
1.07
1.08
3.08
4.08

7l

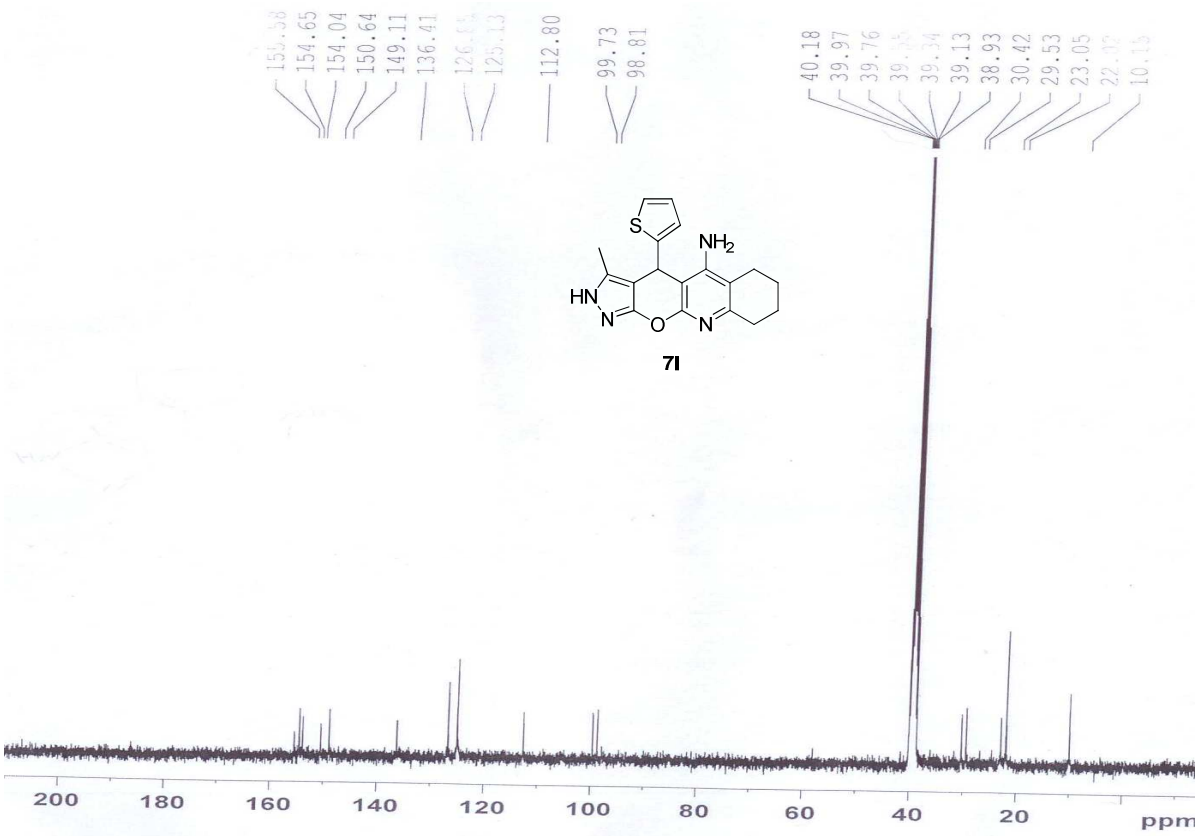

7l